

Summer School on Operational Research and Applications

Inverse Problems in Electromagnetism: Applications
to Plasma Control in Nuclear Fusion Devices

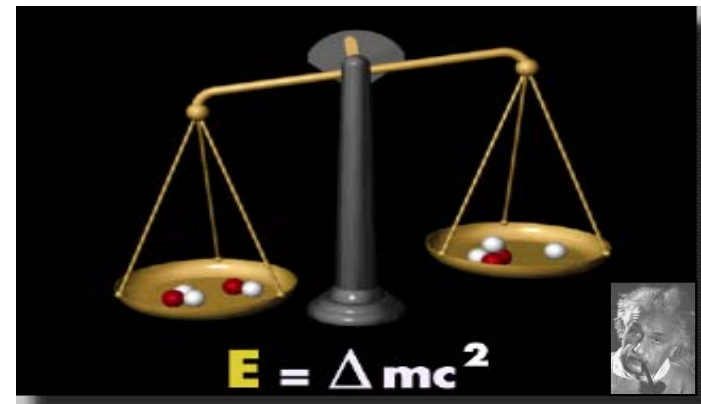
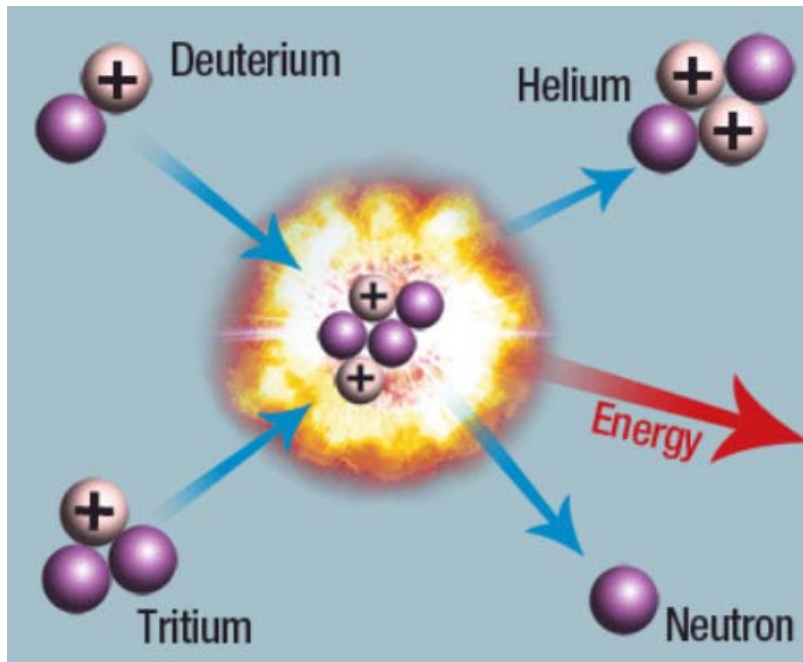
Special session from participants of the ERASMUS PLUS
cooperation project between HSE NN, Russia and University of
Tuscia, Italy

Simone Minucci

- Overview on Nuclear Fusion physics and technology
- Inverse Problems in Nuclear Fusion
- Non-Axisymmetric Flux Density Field Identification
- Magnetic Field Lines Tracing and Plasma Boundary Reconstruction
- Results and next steps
- Conclusions

Nuclear Fusion

Nuclear fusion is a nuclear reaction where two light nuclei (e.g. hydrogen and its isotopes) fuse into a heavier nucleus with a subsequent energy release.



Nuclear Fusion powers the stars

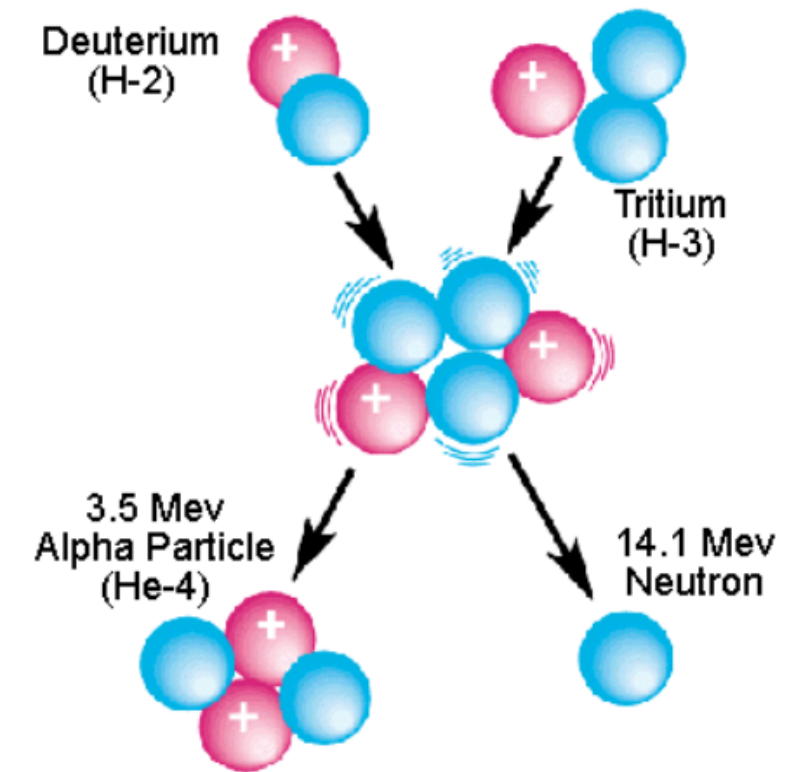
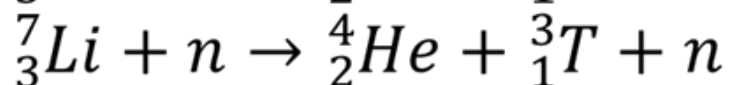
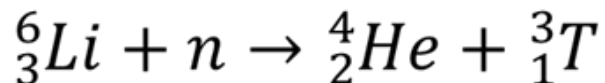


D-T reactions

The easiest fusion reactions to have in a fusion reactor are those involving hydrogen and its isotopes:

- $D + T \rightarrow {}^4\text{He} + n$
- $D + D \rightarrow {}^3\text{He} + n$
- $T + T \rightarrow {}^4\text{He} + 2n$

Deuterium is widely spread on Earth (water) but tritium is not; it can be produced in situ by chemical reactions between electrons and lithium.

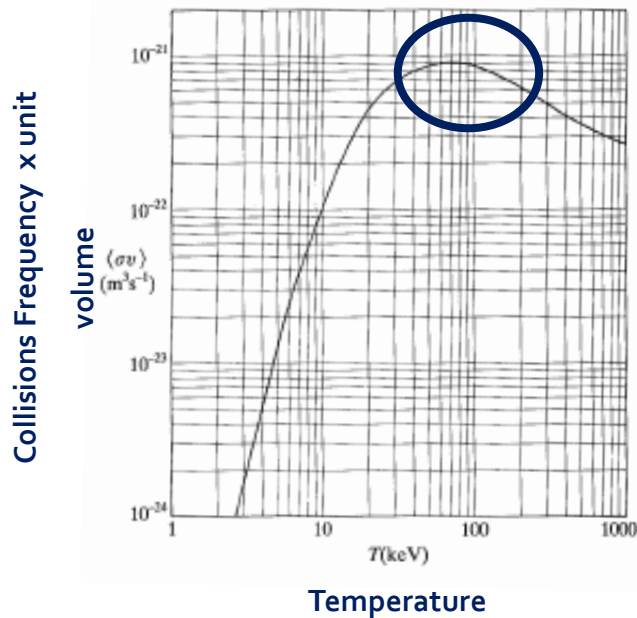


Deuterium-Tritium Fusion Reaction

The plasma

Fusion reagents need to interact at very close distance (sub-atomic distance) in order to let fusion take place.

Fusion reagents need to be energized in order to overcome the Coulomb barrier and let **high speed collisions** take place.



Temperature up to

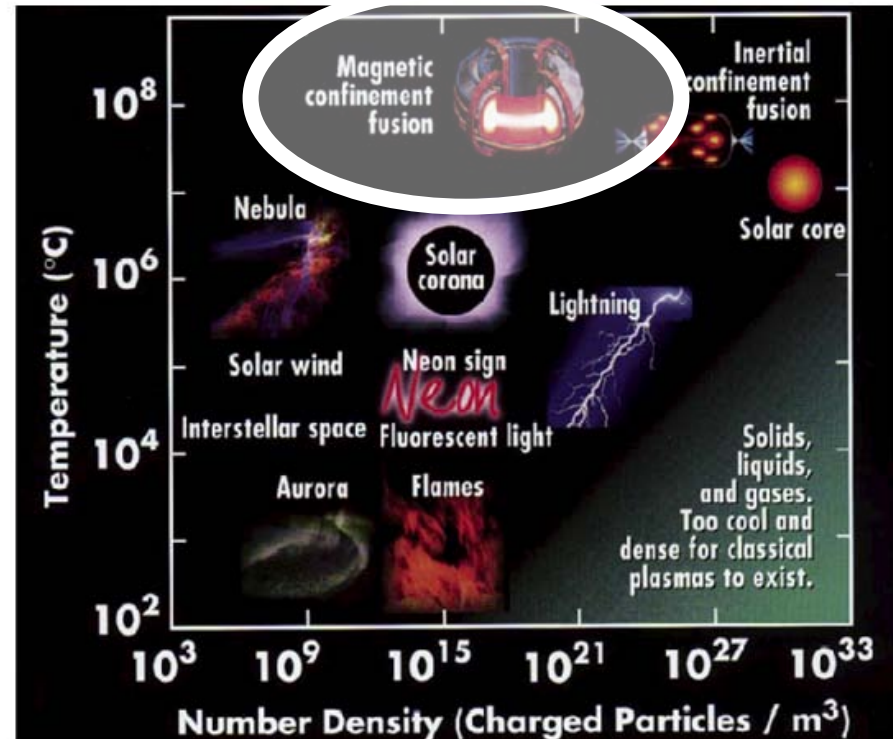
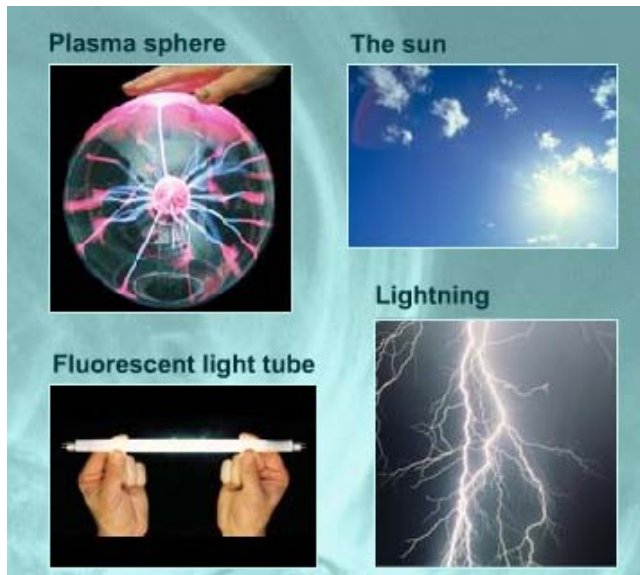
100 millions °C



D-T mixture becomes

PLASMA

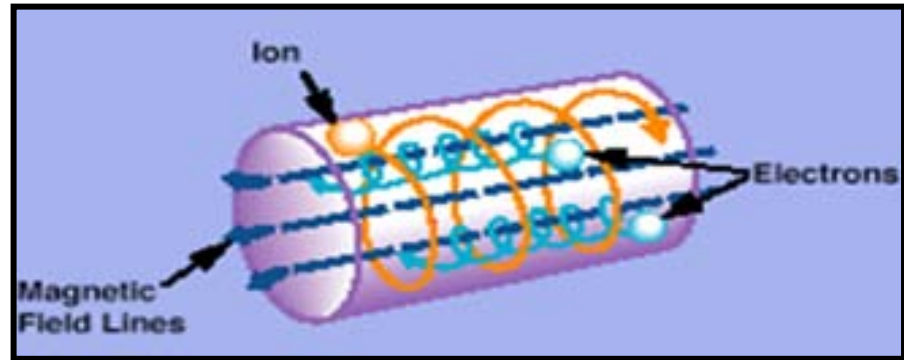
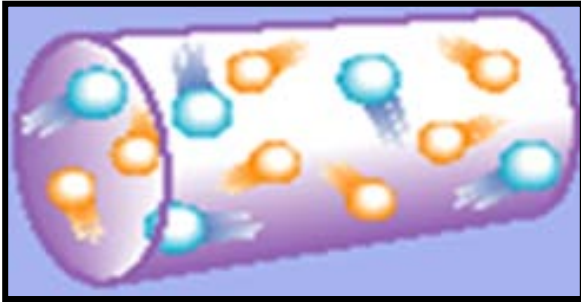
Plasmas are everywhere...



How to produce such a hot plasma?

Where can we confine such a hot plasma?

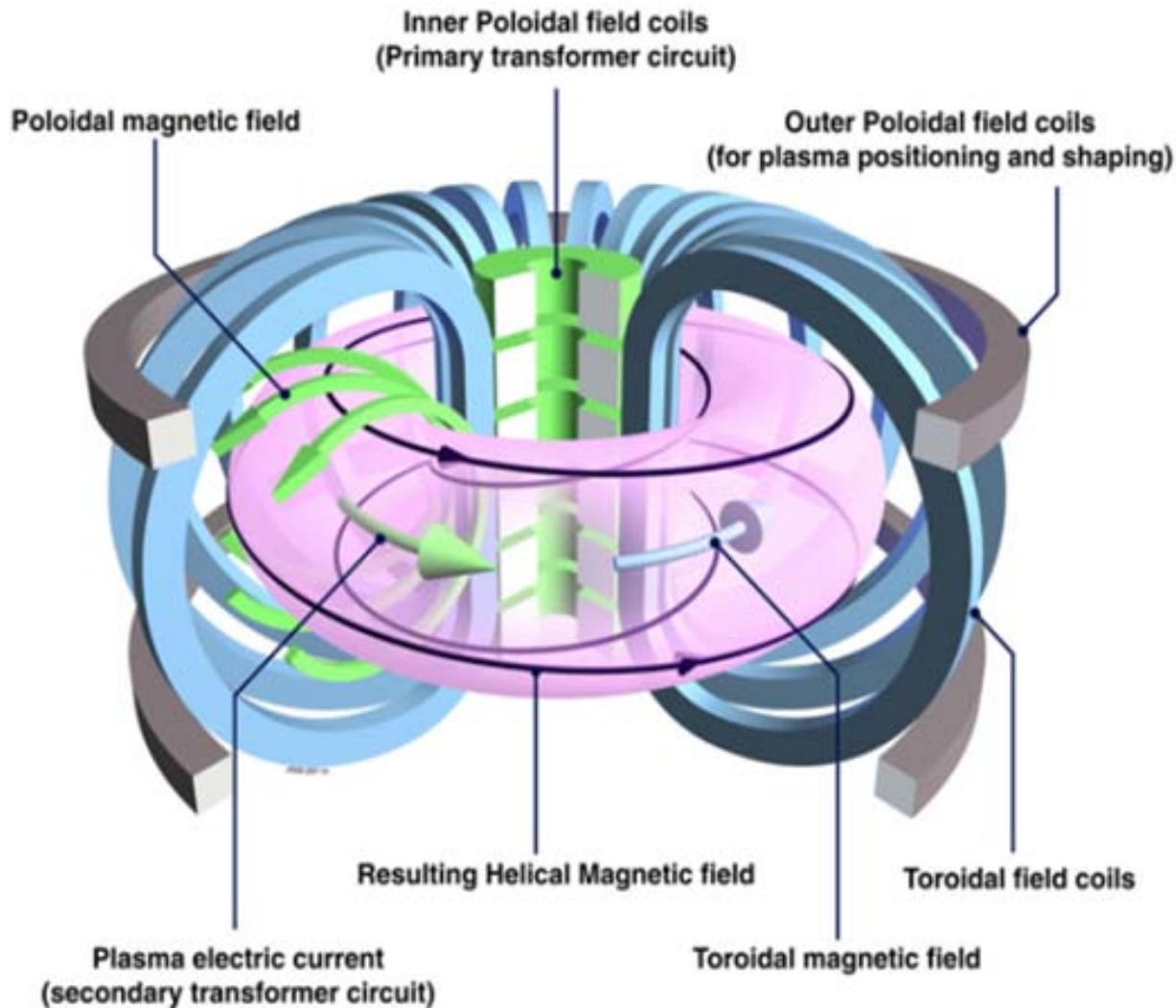
Magnetic Confinement



→ When a **magnetic field** is applied, charged particles are not free to move anymore but **they move on a spiral** along the magnetic field line.

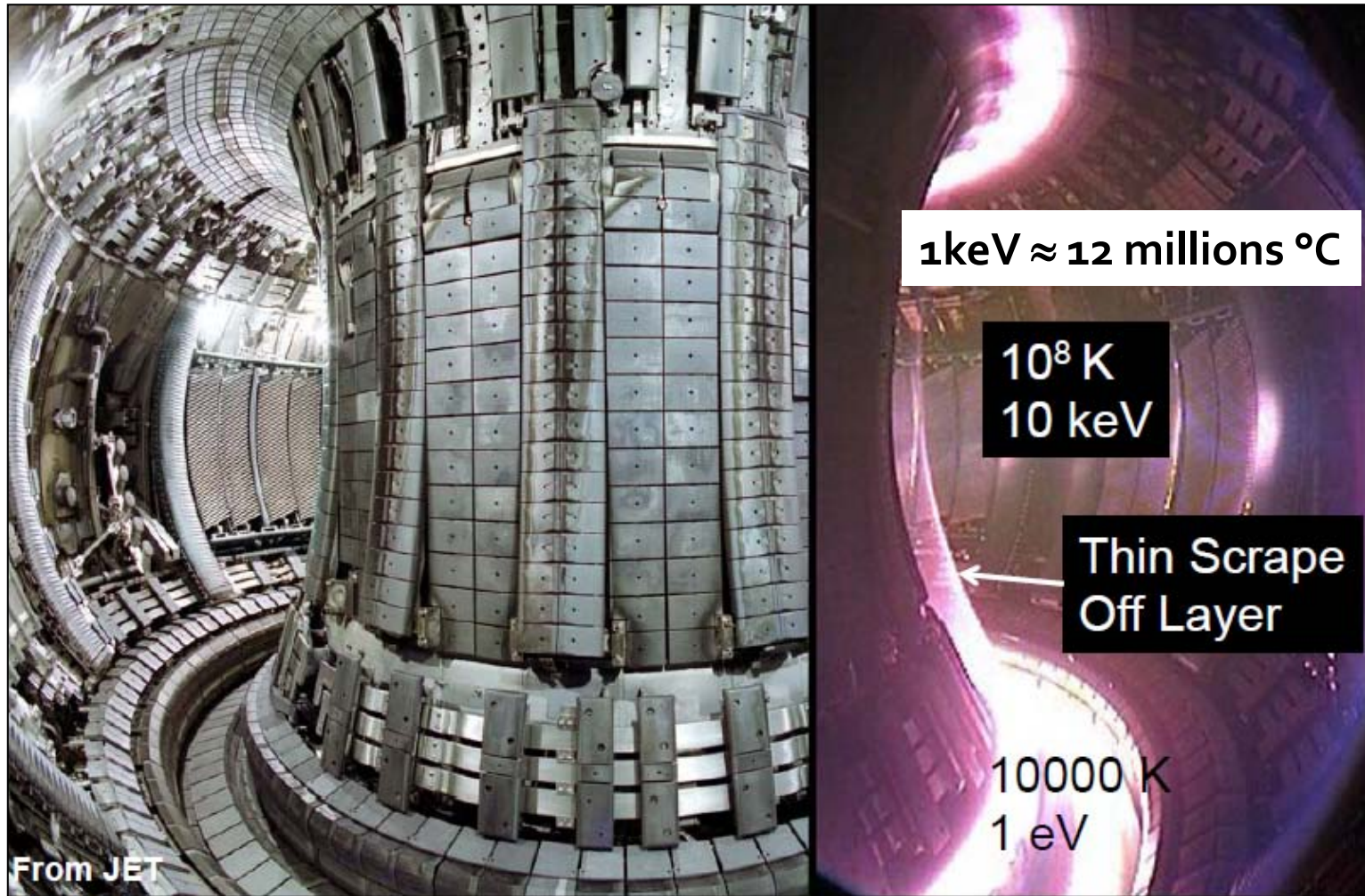
→ In this way, it is possible to **confine the plasma** and avoid it from touching the surrounding structures.

Magnetic Confinement of the plasma

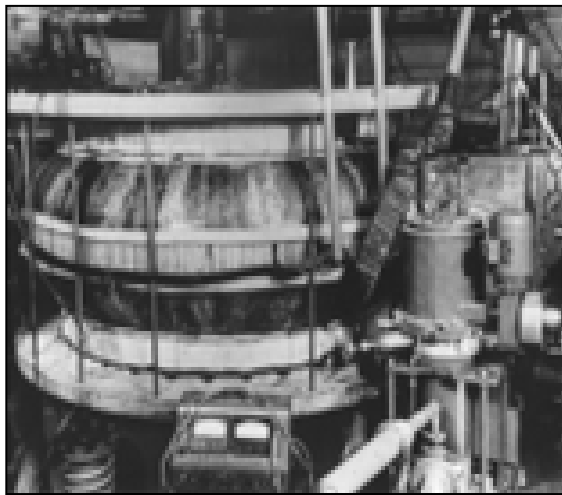


The Tokamak

Торoidalная камера с магнитными катушками

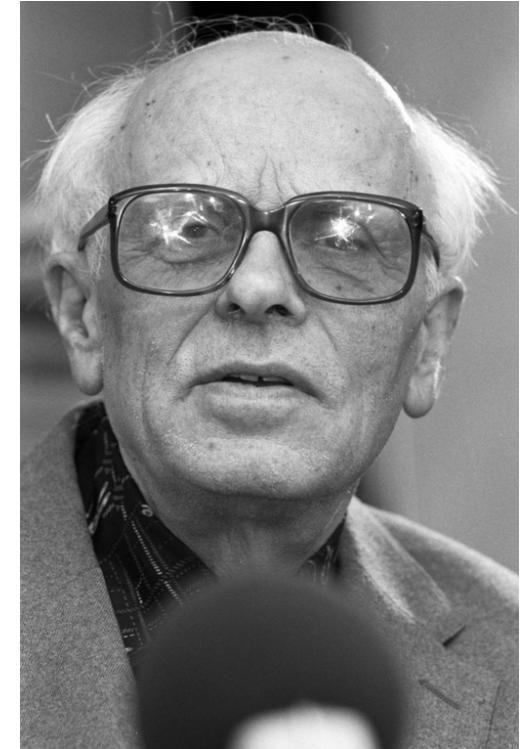


Andrei Sakharov in Нижний Новгород



Russian tokamak T1 (1955)

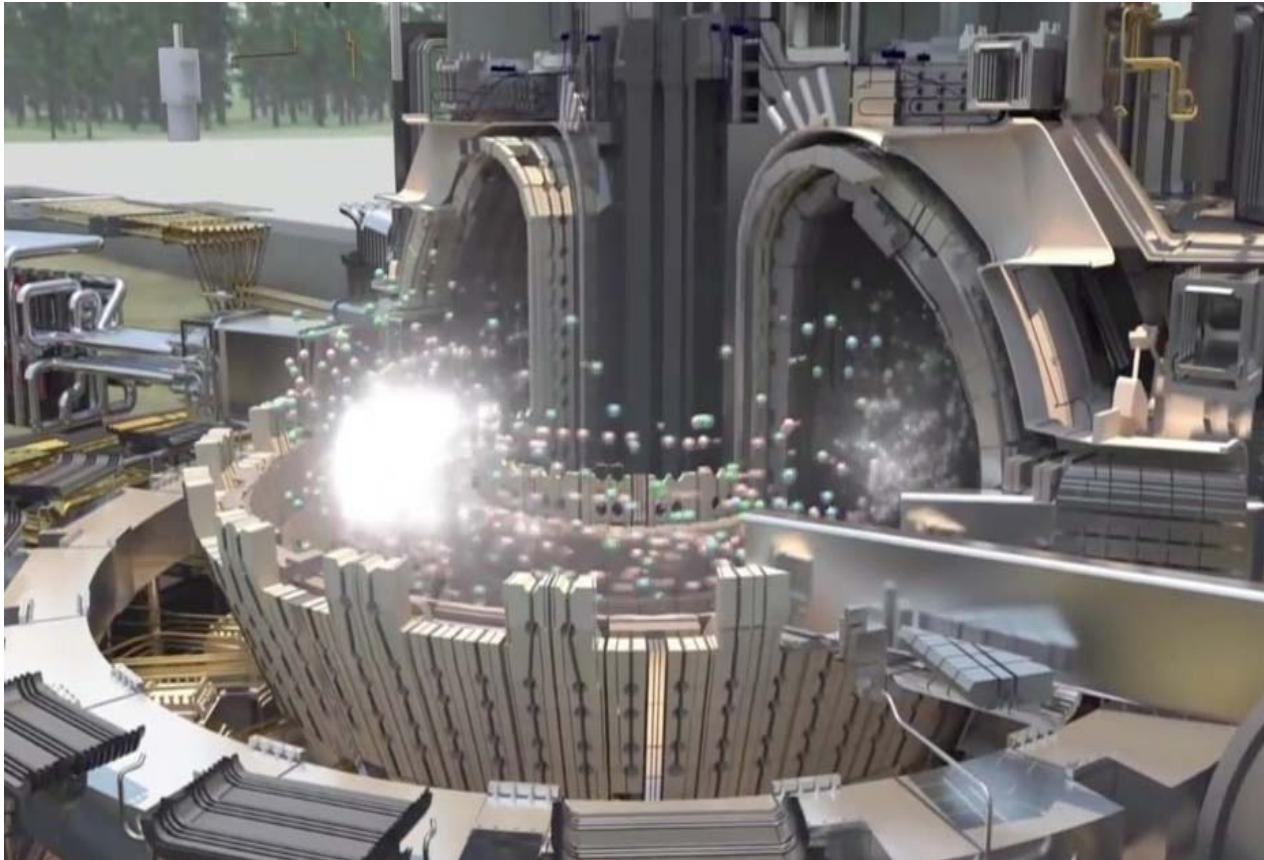
The Tokamak was invented in the 50_{ies} by the russian physicist **Andrei Sakharov** (Nobel prize for peace in 1975)



Нижний Новгород
The physicist and Nobel laureate Andrei Sakharov was exiled there during 1980-1986 to limit his contacts with foreigners.

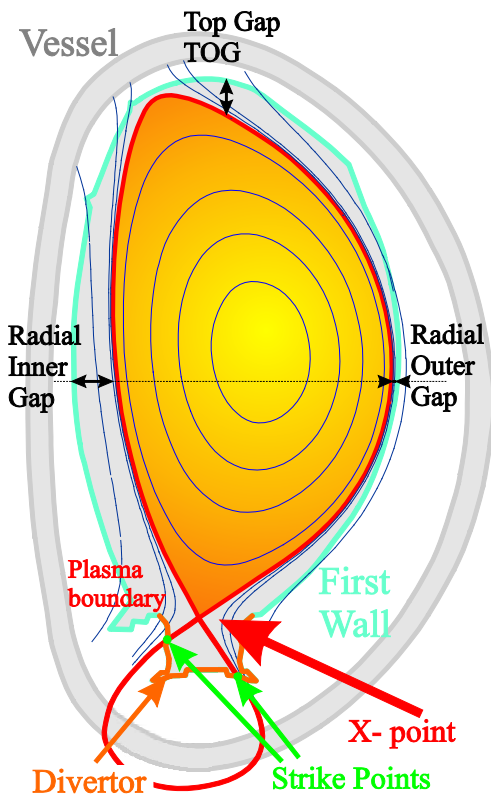
https://en.wikipedia.org/wiki/Nizhny_Novgorod

The Tokamak



(visualization courtesy of Jamison Daniel, Oak Ridge Leadership Computing Facility)

Why a Plasma Boundary Identification



The plasma geometrical parameters (e.g. plasma-wall gaps) are not directly measurable. It is only possible to recover the information regarding the magnetic field distribution inside the vacuum vessel, provided by the magnetic measurements.

A Plasma Identification is essential

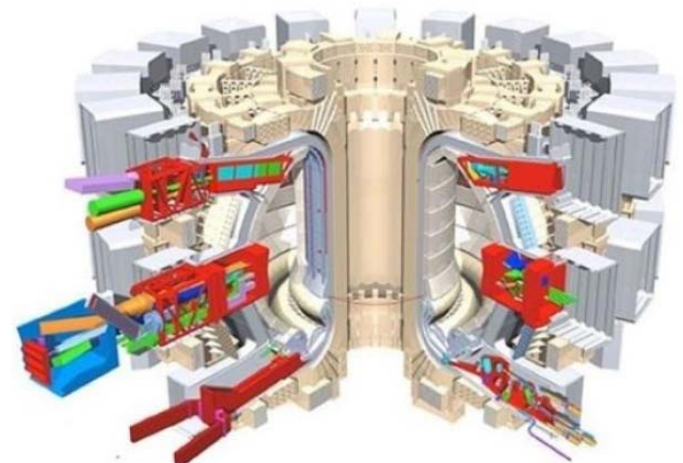
Why a 3D Plasma Boundary Identification



3D symmetry-breaking effects are present in all toroidal fusion configurations because of:

- General Tokamak Engineering
 - Finite number of TF coils, ferrous steel structures (blankets, beams, etc.), error fields from fabrication tolerances
 - Particle/energy sources not symmetrically distributed (pellets, beams, RF)
 - Coils further from plasma, but ports/non-uniformity like in surrounding ferritic steel structures
- Plasma control
 - Coils to control ELMs, RWMs, ...

Advances in 3D simulation tools and diagnostics are mandatory



Inverse Problems in Nuclear Fusion – 1/2



Starting from the measurements, a B field map inside the chamber is reconstructed

Measurements

Magnetic
Modeling

Inverse
Problem Solution

Plasma Boundary

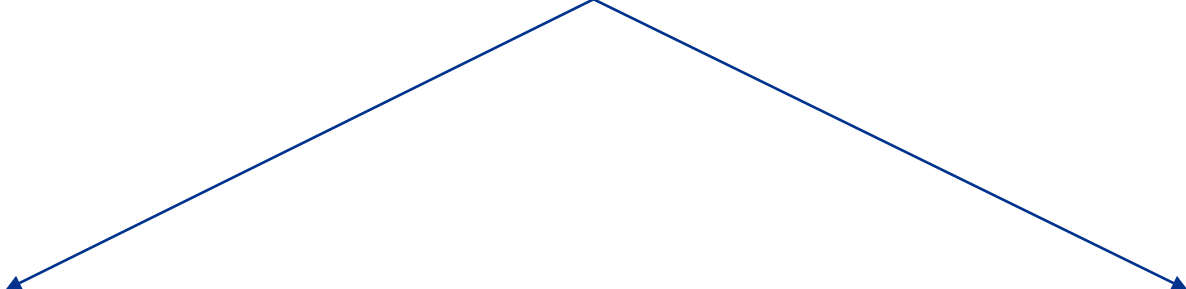
Information on the Plasma Boundary can be obtained from the knowledge of the B field map (e.g: gaps)

Inverse Problems in Nuclear Fusion – 2/2



2D axisymmetric B field	Full 3D B field
Exploitability of analytical surface invariants (e.g. poloidal flux)	Analytical expression of invariants are not known a-priori but in few simple cases (e.g. Clebsch Potentials)
Axisymmetric active currents (simple to be simulated)	3D magnetic sources (Toroidal Field Coils, Error Field Correction Coils, that need a high computational burden)
Axisymmetric plasma current	3D plasma current

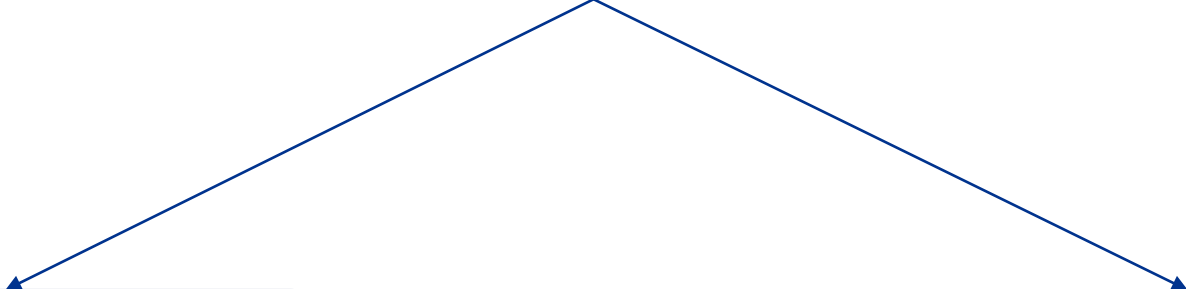
Two approaches have been proposed:



Basis functions to
expand equivalent
sources

Basis functions to
expand the 3D field

Two approaches have been proposed:



Basis functions to
expand equivalent
sources

Basis functions to
expand the 3D field

The magnetic measurements are known just in a discrete set of points, corresponding to the field sensors



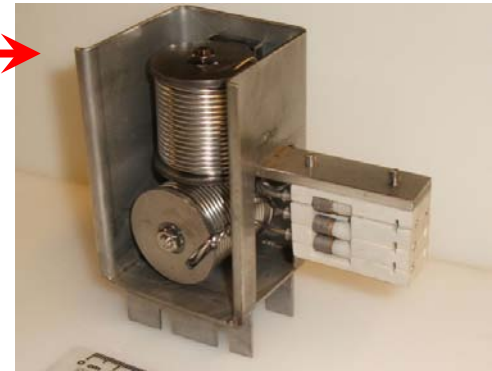
Triaxial Pick-up Coil for magnetic flux density field measurement (Courtesy of EFDA-JET)

3-D Plasma Identification

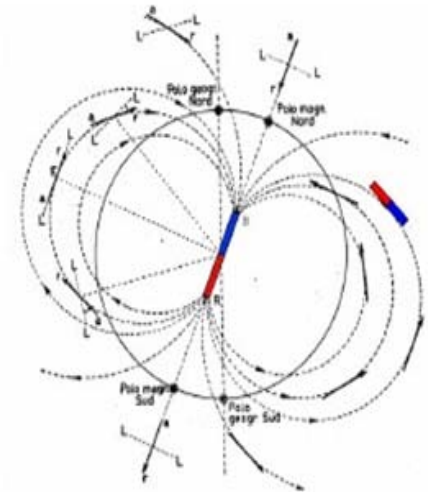
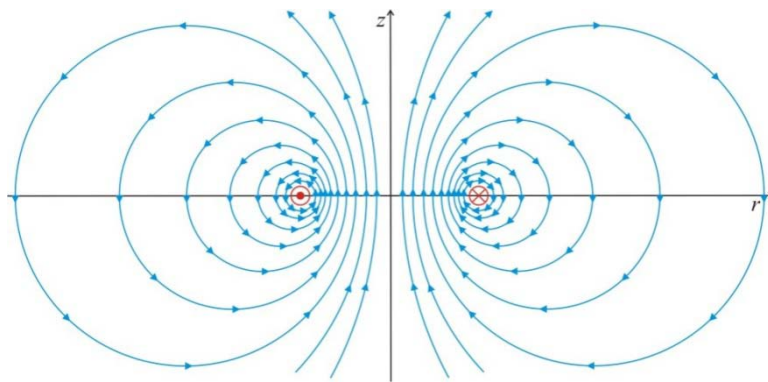
I: 3D Magnetic Field Identification 2/4

Knowledge of the sensors measurements

Definition of a set of basis functions,
by defining a set of equivalent magnetic sources:



Courtesy of EFDA-JET



$$\psi(r, z) = \frac{\mu_0}{\pi} \sum_{n=1}^{N_{fil}} I_n \frac{\sqrt{r r_n'}}{k_n} \left[\left(1 - \frac{k_n^2}{2} \right) K(k_n^2) - E(k_n^2) \right]$$

$$\mathbf{B} = \nabla \psi \times \nabla \phi$$

$$\mathbf{B} = \frac{\mu_0}{4\pi|\mathbf{r}|^3} \left(\frac{3\mathbf{r}(\mathbf{m} \cdot \mathbf{r})}{|\mathbf{r}|^2} - \mathbf{m} \right)$$

Determination of the geometry and the magnitude of each source

I: 3D Magnetic Field Identification 3/4



Problem:

The relation between flux density and geometry of sources is non linear.

Solution:

Fix source geometry (axisymmetric filaments) with axisymmetric currents and sinusoidal distribution of magnetic moments



Observation:

The relation between the flux density field and the magnitude of each source is now linear: the superposition principle can be used

I: 3D Magnetic Field Identification 4/4



$$\begin{bmatrix} m_1 \\ \vdots \\ m_{N_s} \end{bmatrix} = \begin{bmatrix} g_{11} & \cdots & g_{1N_f} \\ \vdots & \ddots & \vdots \\ g_{N_s 1} & \cdots & g_{N_s N_f} \end{bmatrix} \cdot \begin{bmatrix} A_1 \\ \vdots \\ A_{N_f} \end{bmatrix}$$

Measures
Vector

Green
Matrix

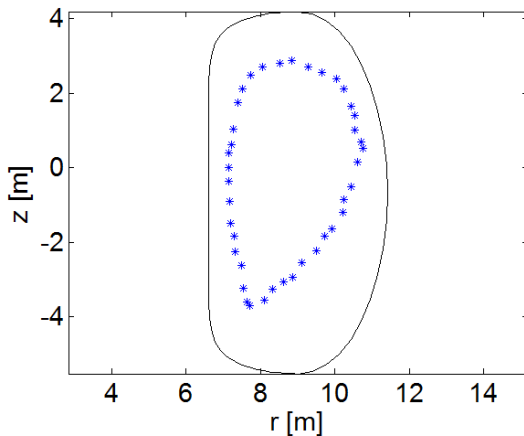
Unknown
Source
Magnitude

g_{ij} is the value of the measure carried out by the i -th sensor when the only j -th source is active with a unit magnitude.

$$\underline{\underline{A}} = \text{pinv}(\underline{\underline{G}}) \cdot \underline{\underline{m}}$$

$$N_{sv} = \frac{N_f}{2}$$

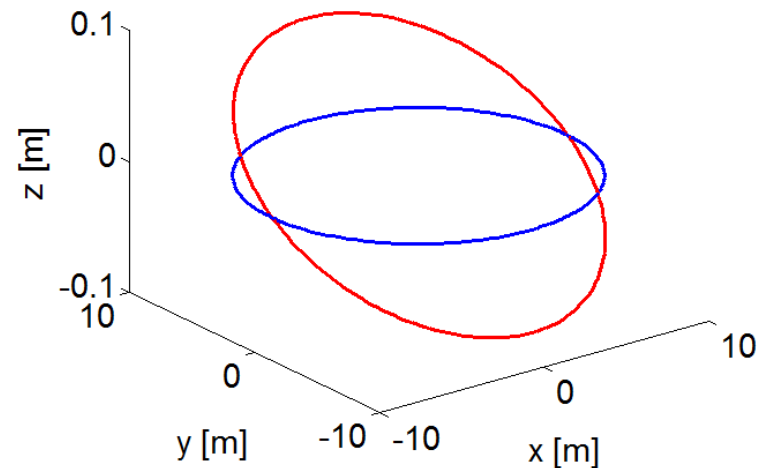
Test Case Definition



Reference:
Axisymmetric equilibrium

Non-axisymmetric perturbation of the filamentary currents:

- 5 cm displacement along the x axis
- 0,5 deg rotation around the x axis

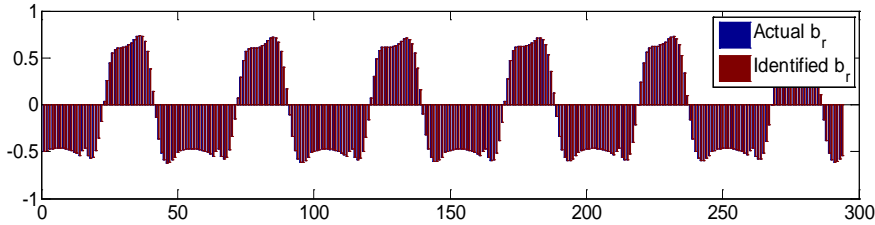


DOFs ($7 \cdot N_{fil}$):

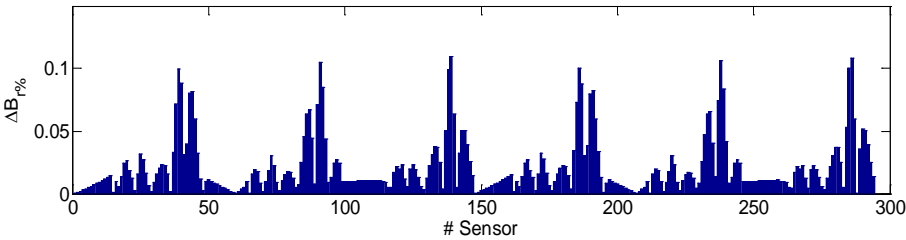
- N_{fil} axisymmetric filamentary currents
- N_{fil} amplitudes & N_{fil} phases for the \mathbf{m}_r distribution
- N_{fil} amplitudes & N_{fil} phases for the \mathbf{m}_z distribution
- N_{fil} amplitudes & N_{fil} phases for the \mathbf{m}_ϕ distribution

Flux Density Field Identification

Radial Field Identification

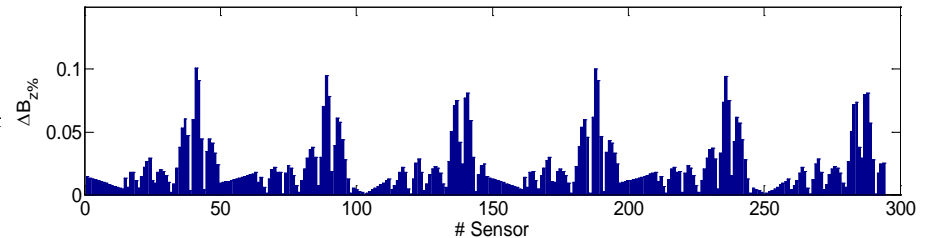
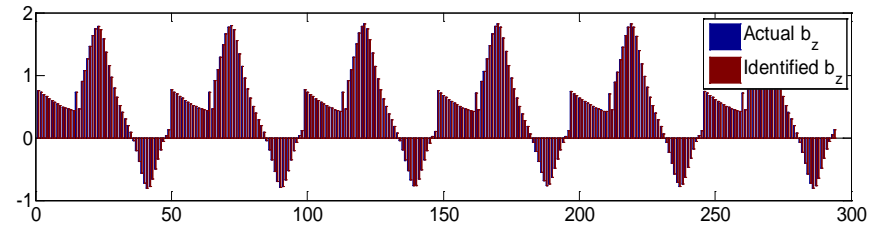


$$\Delta B_{r\%} = 0,0211\%$$

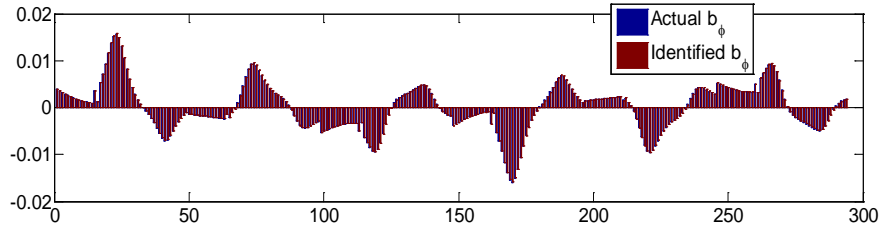


$$\Delta B_{z\%} = 0,0214\%$$

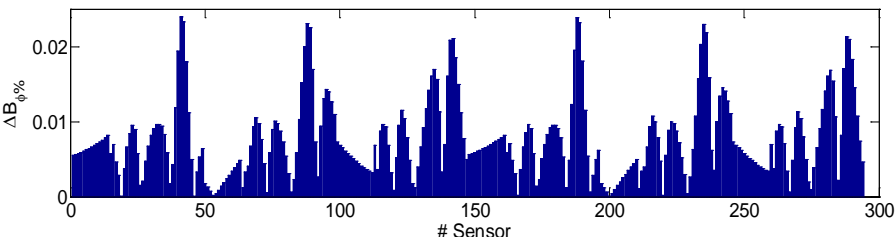
Vertical Field Identification



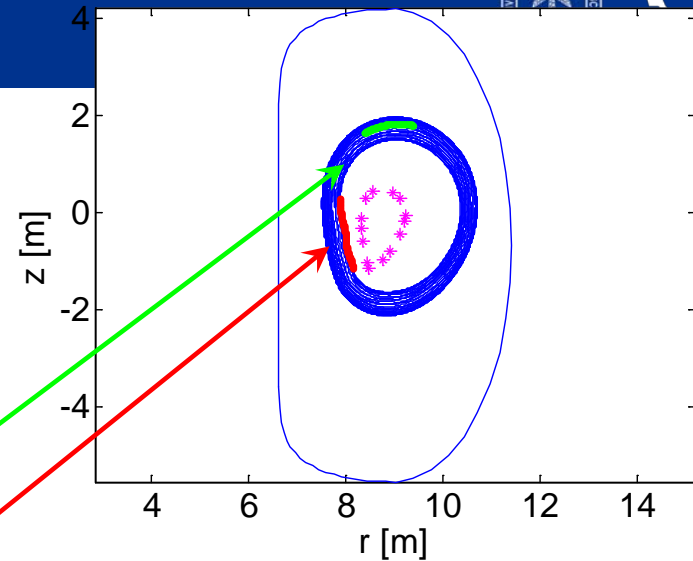
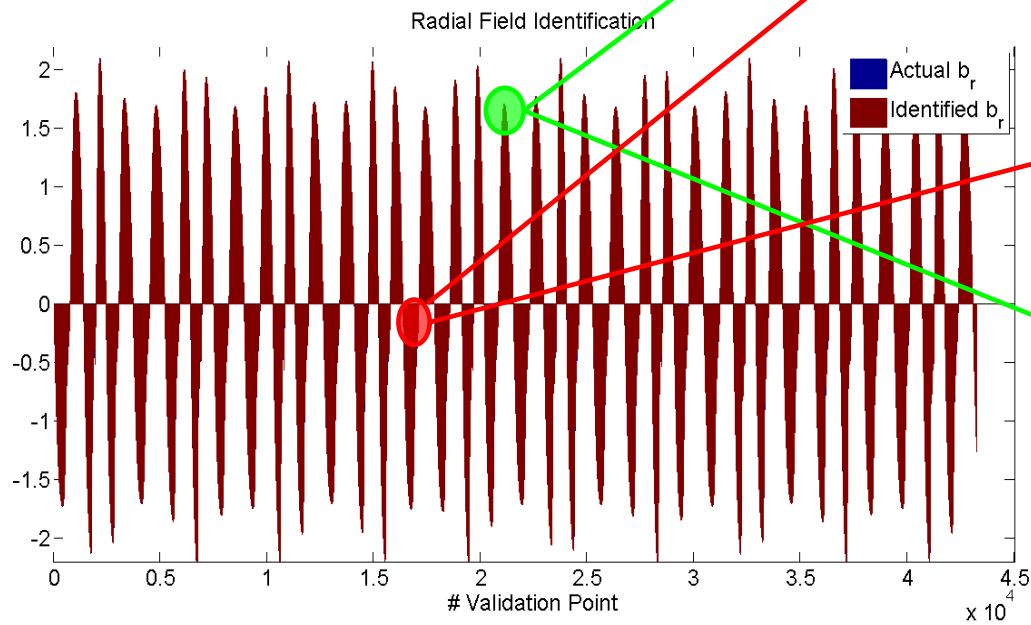
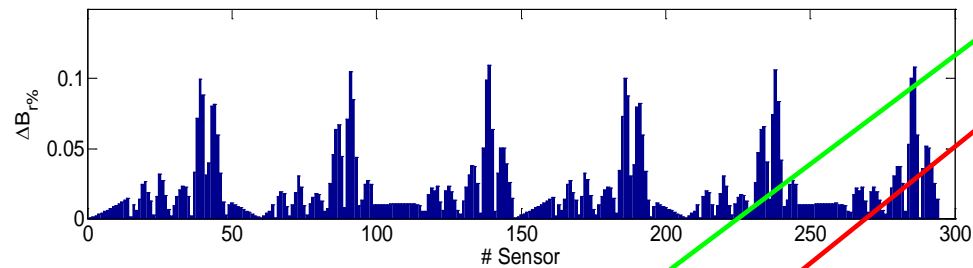
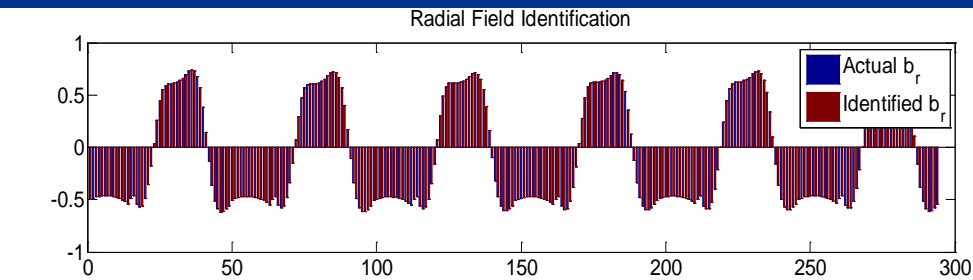
Toroidal Field Identification



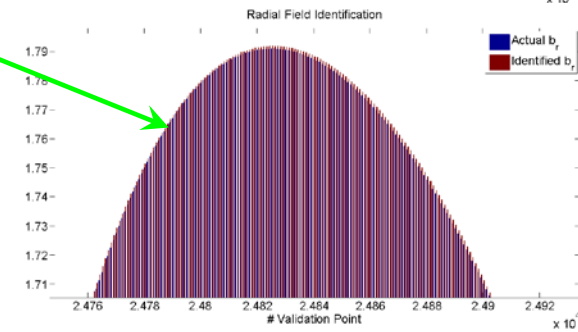
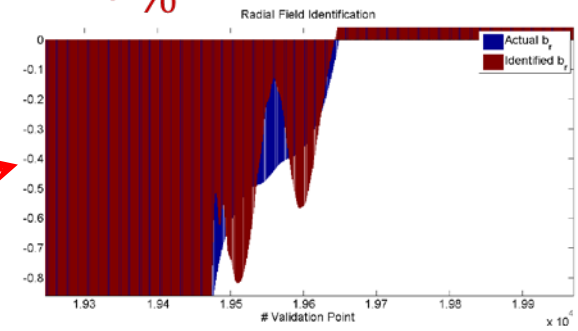
$$\Delta B_{\phi\%} = 0,0076\%$$



Radial Field Identification



$$\Delta B_r \% = 0,0211\%$$



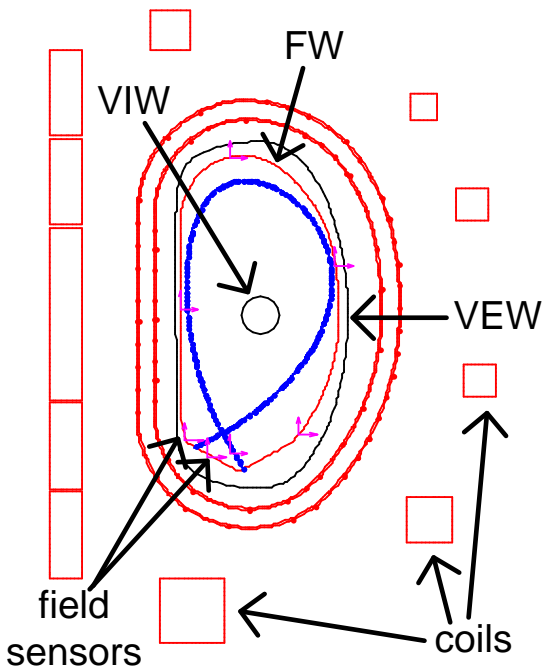
Two approaches have been proposed:

Basis functions to
expand equivalent
sources

Basis functions to
expand the 3D field

II: Magnetic Modeling – VIW & VEW

$$\mathbf{B} = \mathbf{B}_{int} + \mathbf{B}_{ext} + \mathbf{B}_{source}$$



- \mathbf{B}_{int} : solution of a differential problem where the b.c. are given on the VIW. \mathbf{B}_{int} is generated by the plasma
- \mathbf{B}_{ext} : solution of a differential problem where the b.c. are given on the VEW. \mathbf{B}_{ext} is generated by all the unknown sources located outside the plasma (e.g. eddy currents in the Vacuum Vessel)
- \mathbf{B}_{source} : flux density field generated by the known external sources (e.g. PFCs, TFCs, ...)

VIW: Virtual Internal Wall

VEW: Virtual External Wall

$$\text{Sensors' measurements } \mathbf{B} - \text{Calculated } \mathbf{B}_{source} = \text{Information to be identified } \mathbf{B}_{int} + \mathbf{B}_{ext}$$

II: Magnetic Modeling – Mathematical Formulation

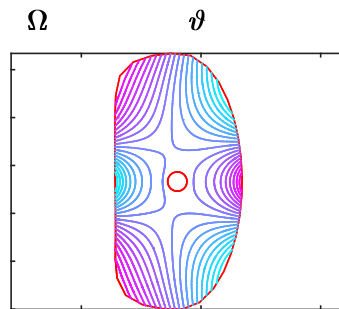
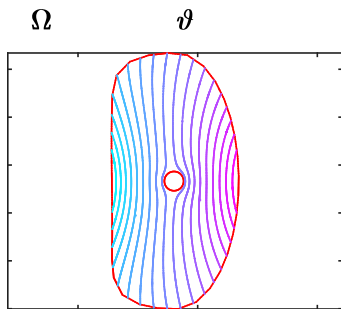


$$\mathbf{B} = \underbrace{\nabla\psi \times \nabla\varphi}_{\substack{\text{Axisymmetric} \\ \text{B field}}} + \underbrace{f_0 \nabla\varphi}_{\substack{\text{Axisymmetric} \\ \text{Toroidal Field}}} \underbrace{- \nabla\Omega}_{\substack{\text{3D B field} \\ \text{perturbation}}}$$

$$\begin{cases} -\frac{\partial}{\partial r} \left(\frac{1}{\mu_0 r} \frac{\partial \psi_{int}(r, z)}{\partial z} \right) - \frac{\partial}{\partial z} \left(\frac{1}{\mu_0 r} \frac{\partial \psi_{int}(r, z)}{\partial r} \right) = 0 \\ \psi_{int}|_{VIW} = \psi_i(r, z) \\ \psi_{int}|_{VEW} = 0 \end{cases} \quad \begin{cases} -\frac{\partial}{\partial r} \left(\frac{1}{\mu_0 r} \frac{\partial \psi_{ext}(r, z)}{\partial z} \right) - \frac{\partial}{\partial z} \left(\frac{1}{\mu_0 r} \frac{\partial \psi_{ext}(r, z)}{\partial r} \right) = 0 \\ \psi_{ext}|_{VIW} = 0 \\ \psi_{ext}|_{VEW} = \psi_e(r, z) \end{cases} \quad \psi = \psi_{int} + \psi_{ext}$$

$$\begin{cases} \nabla^2 \Omega_{int}(r, \varphi, z) = 0 \\ \Omega_{int}|_{VIW} = \Omega_i(r, z) \\ \Omega_{int}|_{VEW} = 0 \end{cases} \quad \begin{cases} \nabla^2 \Omega_{ext}(r, \varphi, z) = 0 \\ \Omega_{ext}|_{VIW} = 0 \\ \Omega_{ext}|_{VEW} = \Omega_e(r, z) \end{cases} \quad \Omega = \Omega_{int} + \Omega_{ext} \quad f_0 = \text{const.}$$

Magnetic Modeling – Basis Functions



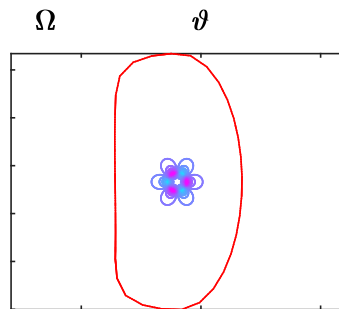
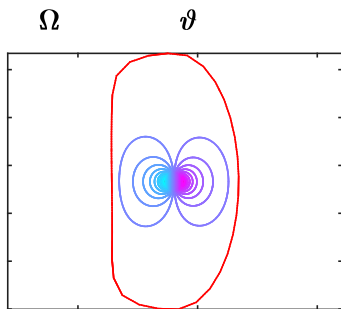
$$\psi_k(r, z) = \sum_{k=1}^{M_\psi} c_k \psi_k(r, z)$$

$$\Omega_k(r, \varphi, z) = \sum_{m=1}^{M_\Omega} \sum_{n \in S} (a_{mn} \cos n\varphi + b_{mn} \sin n\varphi) \cdot \Omega_{mn}(r, z)$$

$$S = \{s_k\}$$

are numerical solution of $\nabla \times \nabla \psi_k \times \nabla \varphi = 0$ when expanding the **boundary conditions** for ψ in Fourier series on the virtual axisymmetric walls

ψ_k



Ω_{mn}

are numerical solution of $\nabla \cdot \nabla \Omega_{mn} = 0$ when expanding the **boundary conditions** for Ω in Fourier series on the virtual axisymmetric walls

Inverse Problem



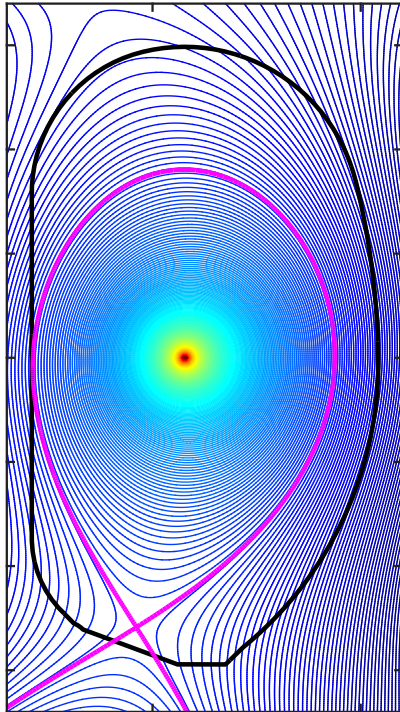
$$\begin{bmatrix} m_1 \\ \vdots \\ m_{N_s} \end{bmatrix} = \begin{bmatrix} g_{11} & \cdots & g_{1N_f} \\ \vdots & \ddots & \vdots \\ g_{N_s 1} & \cdots & g_{N_s N_f} \end{bmatrix} \cdot \begin{bmatrix} A_1 \\ \vdots \\ A_{N_f} \end{bmatrix}$$

Measurements Vector Influence Matrix Unknown vector

Rectangular set of equations, to be solved (for instance) in the least squares sense

g_{ij} is the value of the measurement carried out by the i -th sensor when the only j -th source is active with an unitary magnitude. The unknown vector is defined by the amplitudes a_k, b_k, c_k of the terms in the ψ/Ω series expansion.

Axisymmetric single null equilibrium - 1



Axisymmetric single null equilibrium in a tokamak

The magnetic sources to be identified are:

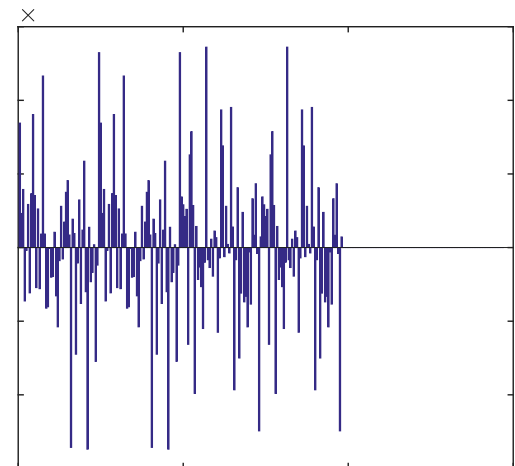
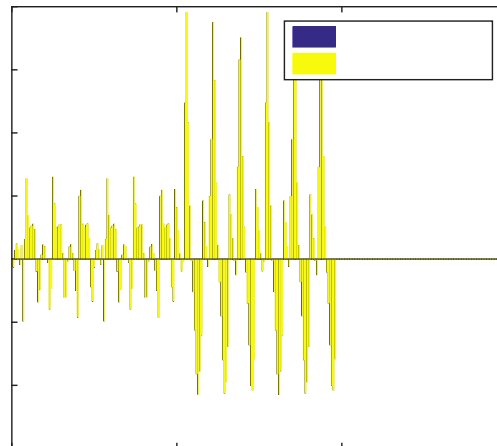
- Current in the Central Solenoid Coils
- Current in the Poloidal Field Coils
- Plasma Current

$$m_{\psi_i} = m_{\psi_e} = 40$$

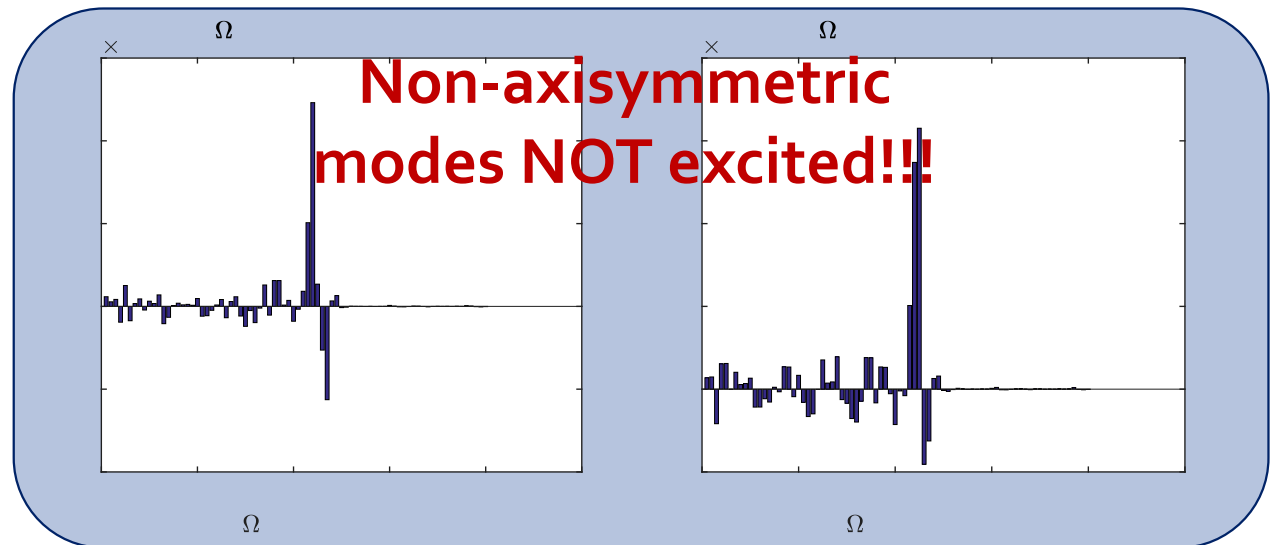
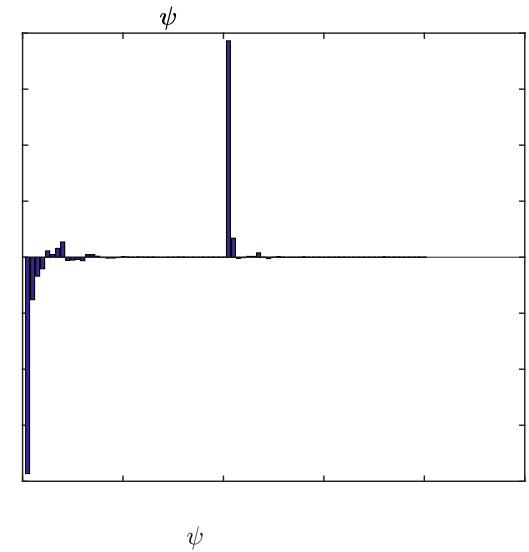
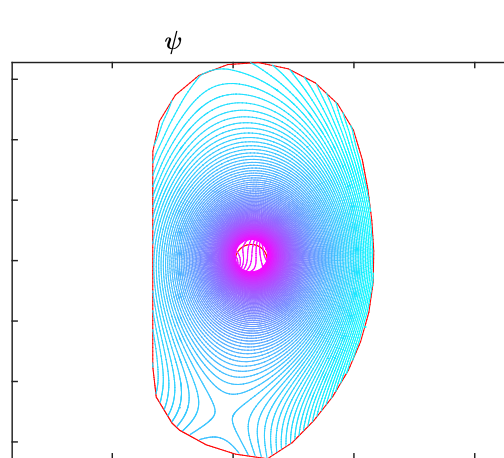
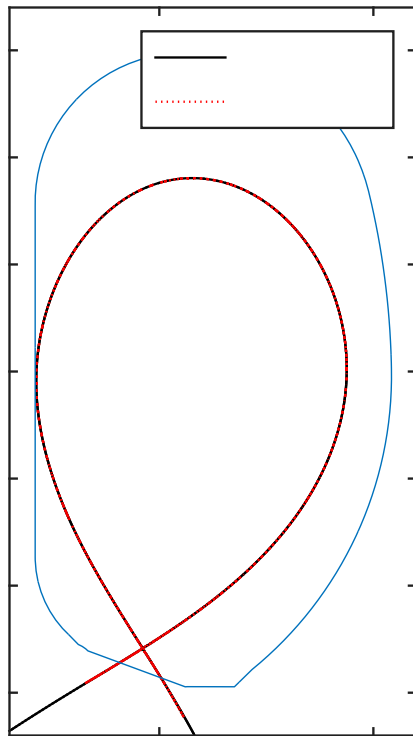
$$m_{\Omega_i} = m_{\Omega_e} = 40, n = 1$$

$$\varepsilon_{fit} = 0,08\%$$

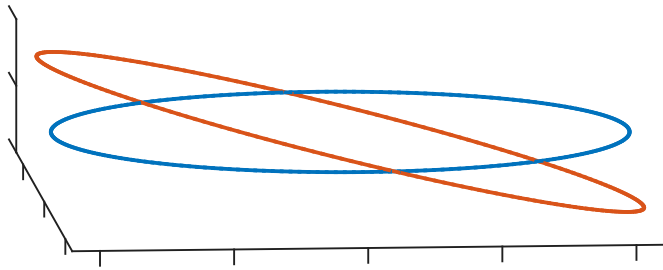
$$\varepsilon_{test} = 0,08\%$$



Axisymmetric single null equilibrium - 2



Kinked Filamentary Current - 1



Axisymmetric current affected by a tilt and shift (kink)

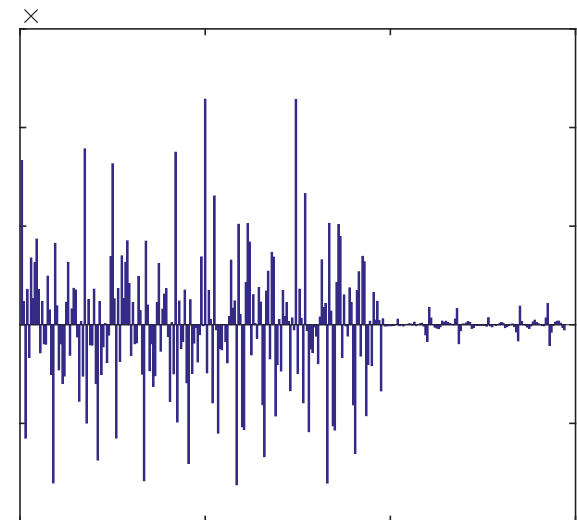
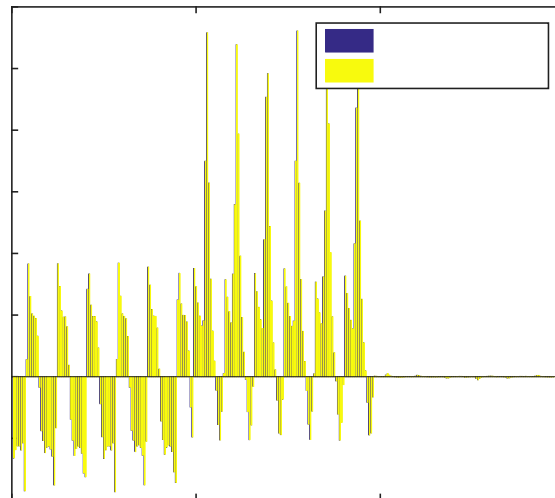
- 2 mm shift along x-axis
- 0,5 deg tilt around x-axis

$$m_{\psi_i} = m_{\psi_e} = 40$$

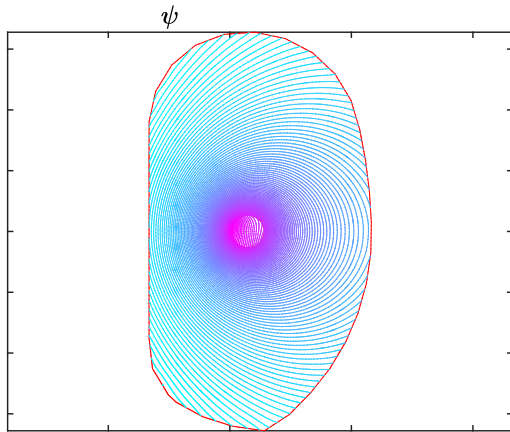
$$m_{\Omega_i} = m_{\Omega_e} = 40, n = 1$$

$$\varepsilon_{fit} = 0,08\%$$

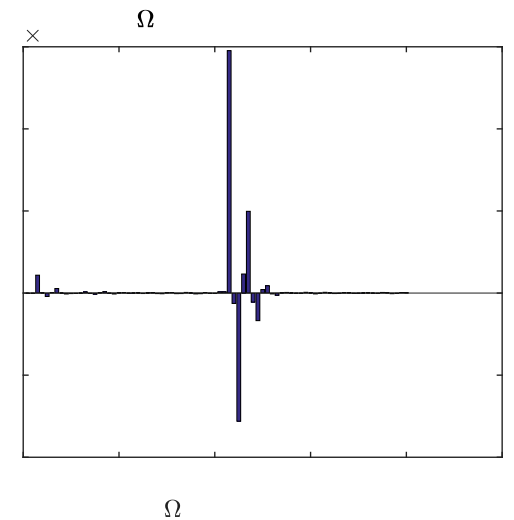
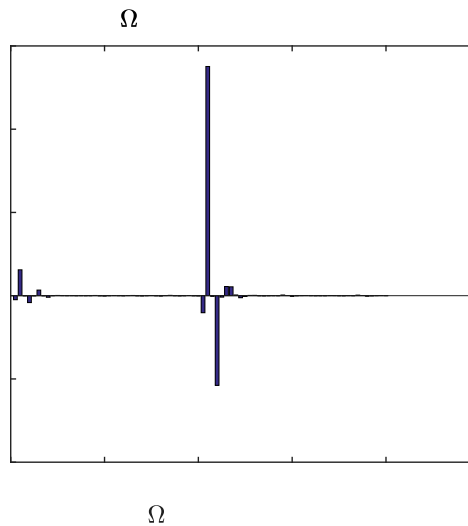
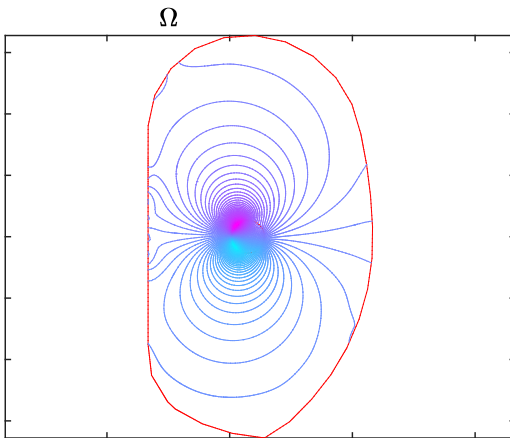
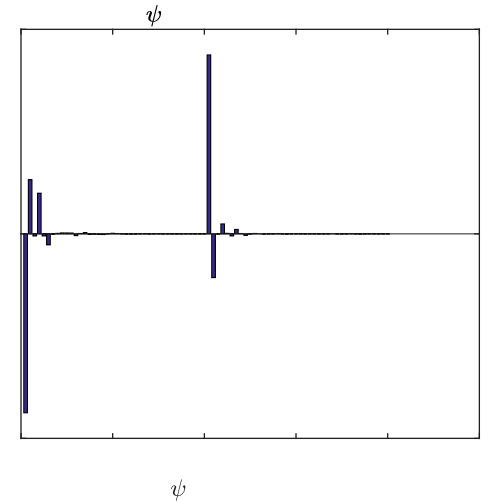
$$\varepsilon_{test} = 0,09\%$$



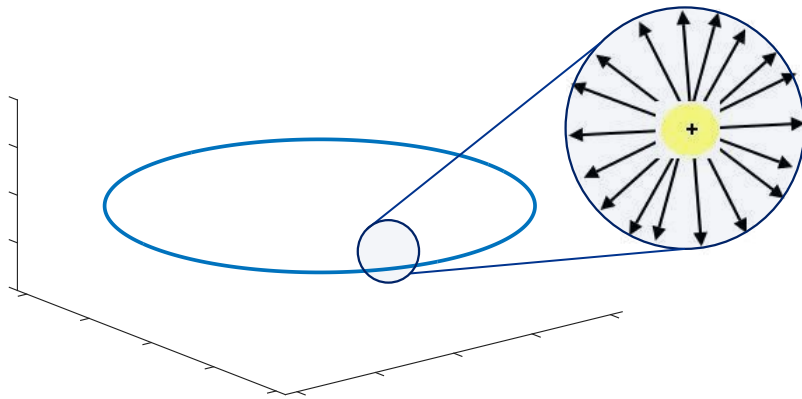
Kinked Filamentary Current - 2



**Axisymmetric modes
are super imposed to
non-axisymmetric n=1
modes**



Sinusoidal magnetic charge distribution on a ring



Axisymmetric «fictitious magnetic» charge distribution.

The amplitude of each charge is modulated by a sine wave of a given spatial frequency along the toroidal direction

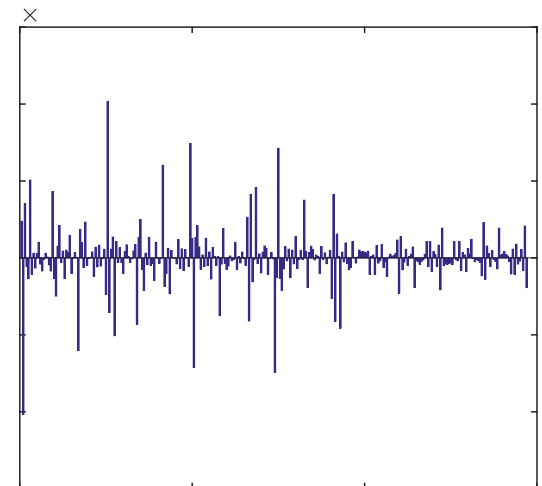
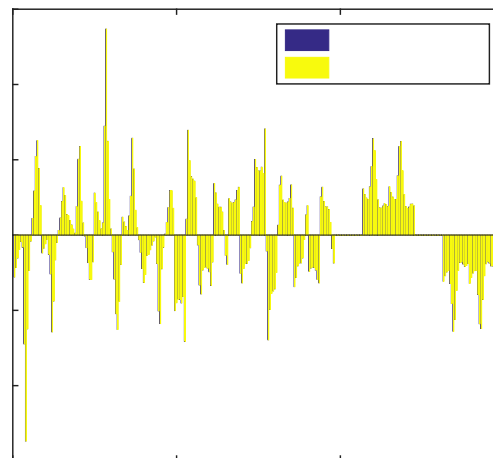
$$m_{\psi_i} = m_{\psi_e} = 40$$

$$m_{\Omega_i} = m_{\Omega_e} = 40, n = 1$$

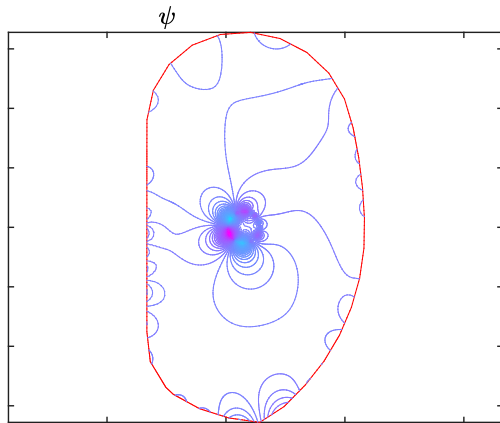
**Analytical $n = 1$
solution is
AVAILABLE!**

$$\varepsilon_{fit} = 0.05\%$$

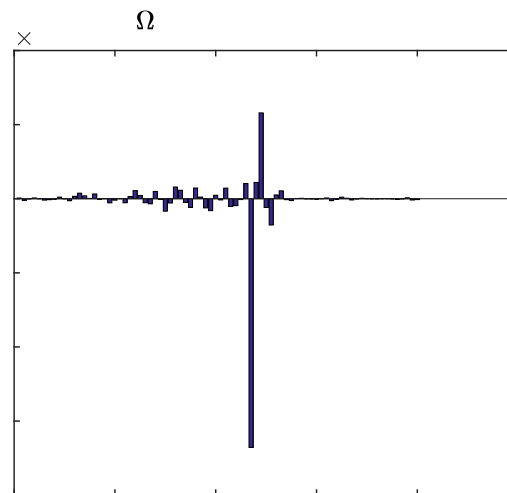
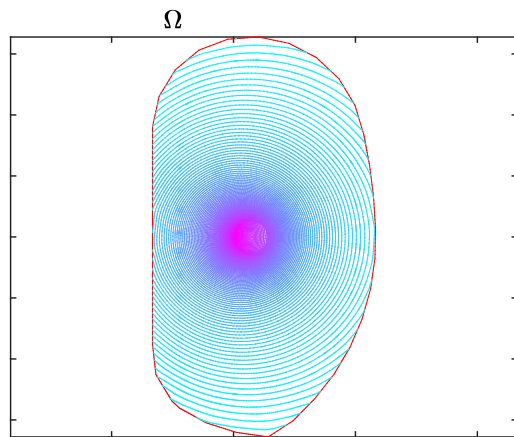
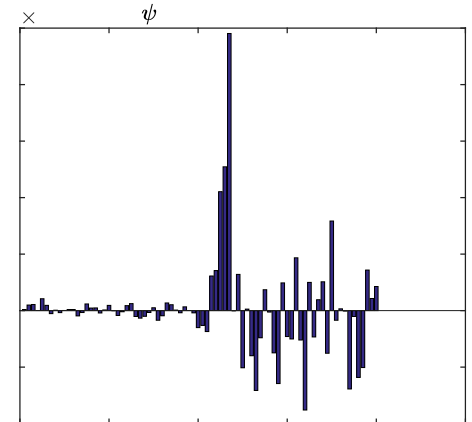
$$\varepsilon_{test} = 0.3\%$$



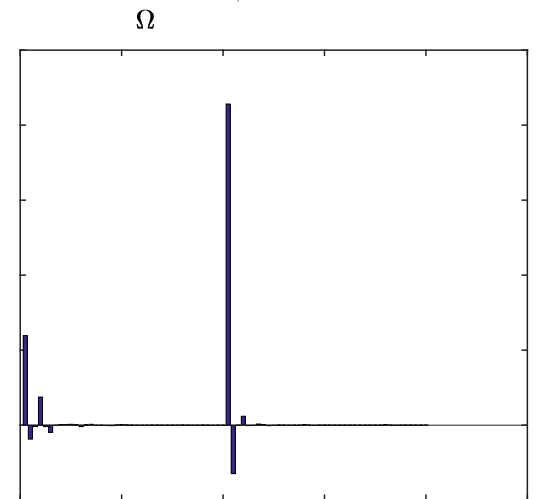
Sinusoidal magnetic charge distribution on a ring - 2



**Axisymmetric modes
not excited!**
**NO information regarding
the symmetry of the field
distribution are provided!!!**

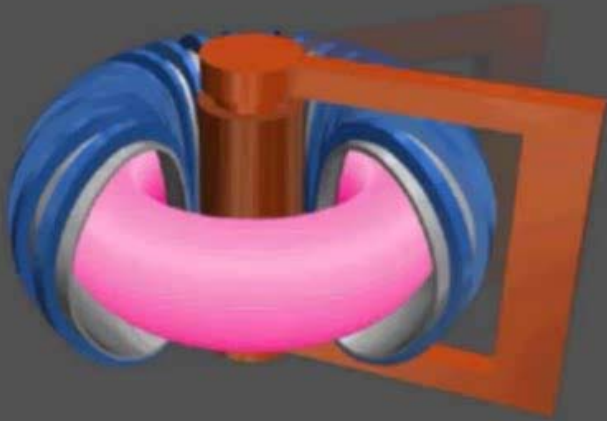


Ω



Ω

Field Lines Tracing



- Plasma particles trajectories
- Plasma-wall gaps
- Plasma behaviour in terms of closed OR ergodic lines
- Connection Lengths
- Heat loads on the divertor and other structure surrounding the structure

$$\begin{cases} \frac{\partial r}{\partial \varphi} = r \frac{B_r}{B_\varphi} \\ \frac{\partial z}{\partial \varphi} = r \frac{B_z}{B_\varphi} \end{cases}$$

$$\nabla \cdot \mathbf{B} = 0$$



$$\frac{d\mathbf{x}}{dt} = \mathbf{B}(\mathbf{x})$$

A numerical integrator is called Geometric Integrator if some qualitative geometrical properties of the dynamic system to be integrated is exactly preserved, such as the Hamiltonian structure of the ODEs (**Symplectic Integrators**).

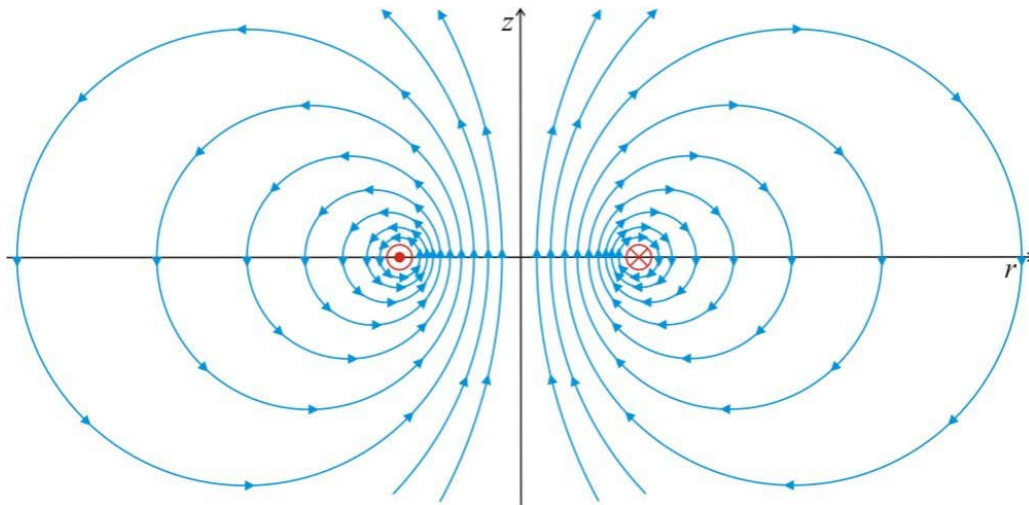
**Magnetic Flux Density
Field Lines tracing**



$$\nabla \cdot \mathbf{B} = 0$$



**Volume
Preserving
Integrators**



Volume Preserving Integrators



A geometric integrator is a Volume Preserving Integrator if it preserves the divergence-free structure of ODEs:

$$\frac{dx}{dt} = B(x) \quad \longleftrightarrow \quad \nabla \cdot B = \sum_{i=1}^N \frac{\partial B_i}{\partial x_i} = 0$$

A chosen unit volume overall the integration of the source-free field is exactly kept constant (like in incompressible fluids, where Lagrangian trajectories coincide with the velocity field lines in stationary conditions).

$$x_{k+1} = \Phi(x_k, x_{k+1}, t_k, t_{k+1}, B_k, B_{k+1}, h)$$

$$\begin{cases} \dot{x} = B_x \\ \dot{y} = B_y \\ \dot{z} = B_z \end{cases} \quad J_\Phi = \begin{bmatrix} \frac{\partial x_{k+1}}{\partial x_k} & \frac{\partial x_{k+1}}{\partial y_k} & \frac{\partial x_{k+1}}{\partial z_k} \\ \frac{\partial y_{k+1}}{\partial x_k} & \frac{\partial y_{k+1}}{\partial y_k} & \frac{\partial y_{k+1}}{\partial z_k} \\ \frac{\partial z_{k+1}}{\partial x_k} & \frac{\partial z_{k+1}}{\partial y_k} & \frac{\partial z_{k+1}}{\partial z_k} \end{bmatrix}$$

$$\det(J_\Phi) = 1$$

The Implicit Mid-Point Rule (MR)



$$\mathbf{x}_{k+1} = \mathbf{x}_k + h \cdot \mathbf{B} \left(\frac{\mathbf{x}_{k+1} + \mathbf{x}_k}{2} \right)$$

In two dimensions, MR discretization is exactly **area preserving**:

$$\frac{\partial \mathbf{x}_{k+1}}{\partial \mathbf{x}_k} = I + h \cdot \frac{\partial}{\partial \mathbf{x}} \mathbf{B}(\mathbf{x}) \Big|_{\frac{\mathbf{x}_{k+1} + \mathbf{x}_k}{2}} \cdot \left(\frac{1}{2} \frac{\partial \mathbf{x}_{k+1}}{\partial \mathbf{x}_k} + \frac{1}{2} I \right)$$

$$J = \left(I - \frac{h}{2} F \right)^{-1} \left(I + \frac{h}{2} F \right) \quad F_{ij} = \frac{\partial B_i}{\partial x_j}$$

$$\det(J) = \frac{1 + \frac{h}{2} \cancel{\text{Tr}(F)} + \frac{h^2}{4} \det(F)}{1 - \frac{h}{2} \cancel{\text{Tr}(F)} + \frac{h^2}{4} \det(F)} = \frac{1 + \frac{h^2}{4} \det(F)}{1 + \frac{h^2}{4} \det(F)} = 1$$

Splitting with Vector Potential 1/2



Problem:

In three dimensions MR discretization is not exactly volume preserving, because the Jacobian determinant is not exactly 1, but approaches to 1 by the cube of the integration step.



Solution:

Generating Function Approach: Splitting of the original divergence-free field using a vector potential to generate three vector fields, whose superposition gives the original field, all of them being 2-D and obviously divergence-free.

$$\mathbf{B} = \nabla \times \mathbf{A} \Rightarrow \begin{cases} \mathbf{B}_1 = \nabla A_x \times \hat{i}_x \\ \mathbf{B}_2 = \nabla A_y \times \hat{i}_y \\ \mathbf{B}_3 = \nabla A_z \times \hat{i}_z \end{cases} \quad \begin{cases} \dot{\mathbf{x}}_1 = \mathbf{B}_1 \\ \dot{\mathbf{x}}_2 = \mathbf{B}_2 \\ \dot{\mathbf{x}}_3 = \mathbf{B}_3 \end{cases}$$

$$\mathbf{B} = \mathbf{B}_1 + \mathbf{B}_2 + \mathbf{B}_3$$

Splitting with Vector Potential 2/2



$$\nabla A_x = \begin{bmatrix} \frac{\partial A_x}{\partial x} \\ \frac{\partial A_x}{\partial y} \\ \frac{\partial A_x}{\partial z} \end{bmatrix} \quad \mathbf{B}_1 = \begin{cases} 0\hat{i}_x \\ \frac{\partial A_x}{\partial z}\hat{i}_y \\ -\frac{\partial A_x}{\partial y}\hat{i}_z \end{cases} \quad \begin{cases} \frac{dy}{d\tau} = \frac{\partial A_x}{\partial z} \\ \frac{dz}{d\tau} = -\frac{\partial A_x}{\partial y} \end{cases}$$

$$\nabla A_y = \begin{bmatrix} \frac{\partial A_y}{\partial x} \\ \frac{\partial A_y}{\partial y} \\ \frac{\partial A_y}{\partial z} \end{bmatrix} \quad \mathbf{B}_2 = \begin{cases} -\frac{\partial A_y}{\partial z}\hat{i}_x \\ 0\hat{i}_y \\ -\frac{\partial A_y}{\partial x}\hat{i}_z \end{cases} \quad \begin{cases} \frac{dx}{d\tau} = -\frac{\partial A_y}{\partial z} \\ \frac{dz}{d\tau} = \frac{\partial A_y}{\partial x} \end{cases}$$

$$\nabla A_z = \begin{bmatrix} \frac{\partial A_z}{\partial x} \\ \frac{\partial A_z}{\partial y} \\ \frac{\partial A_z}{\partial z} \end{bmatrix} \quad \mathbf{B}_3 = \begin{cases} \frac{\partial A_z}{\partial y}\hat{i}_x \\ -\frac{\partial A_z}{\partial x}\hat{i}_y \\ 0\hat{i}_z \end{cases} \quad \begin{cases} \frac{dx}{d\tau} = \frac{\partial A_z}{\partial y} \\ \frac{dy}{d\tau} = -\frac{\partial A_z}{\partial x} \end{cases}$$

**A_x, A_y & A_z :
Hamiltonian
Functions of the
2-D ODE sets**



**2-D ode set
+
Hamiltonian set
=
Area Preserving**

MR Procedure – Cascaded Scheme

$$\begin{cases} x_{k+1}^1 = x_k \\ y_{k+1}^1 = y_k + \frac{h}{2} \cdot B_{1y} \left(x_k, \frac{y_k + y_{k+1}}{2}, \frac{z_k + z_{k+1}}{2} \right) \\ z_{k+1}^1 = z_k + \frac{h}{2} \cdot B_{1z} \left(x_k, \frac{y_k + y_{k+1}}{2}, \frac{z_k + z_{k+1}}{2} \right) \end{cases}$$



$$\begin{cases} x_{k+1}^2 = x_{k+1}^1 + \frac{h}{2} \cdot B_{2x} \left(\frac{x_{k+1}^1 + x_{k+1}^2}{2}, y_{k+1}^1, \frac{z_{k+1}^1 + z_{k+1}^2}{2} \right) \\ y_{k+1}^2 = y_{k+1}^1 \\ z_{k+1}^2 = z_{k+1}^1 + \frac{h}{2} \cdot B_{2z} \left(\frac{x_{k+1}^1 + x_{k+1}^2}{2}, y_{k+1}^1, \frac{z_{k+1}^1 + z_{k+1}^2}{2} \right) \end{cases}$$

$$\begin{cases} x_{k+1}^3 = x_{k+1}^2 + h \cdot B_{3x} \left(\frac{x_{k+1}^2 + x_{k+1}^3}{2}, \frac{y_{k+1}^2 + y_{k+1}^3}{2}, z_{k+1}^2 \right) \\ y_{k+1}^3 = y_{k+1}^2 + h \cdot B_{3y} \left(\frac{x_{k+1}^2 + x_{k+1}^3}{2}, \frac{y_{k+1}^2 + y_{k+1}^3}{2}, z_{k+1}^2 \right) \\ z_{k+1}^3 = z_{k+1}^2 \end{cases}$$



$$\begin{cases} x_{k+1}^4 = x_{k+1}^3 + \frac{h}{2} \cdot B_{2x} \left(\frac{x_{k+1}^3 + x_{k+1}^4}{2}, y_{k+1}^3, \frac{z_{k+1}^3 + z_{k+1}^4}{2} \right) \\ y_{k+1}^4 = y_{k+1}^3 \\ z_{k+1}^4 = z_{k+1}^3 + \frac{h}{2} \cdot B_{2z} \left(\frac{x_{k+1}^3 + x_{k+1}^4}{2}, y_{k+1}^3, \frac{z_{k+1}^3 + z_{k+1}^4}{2} \right) \end{cases}$$



$$\begin{cases} x_{k+1} = x_{k+1}^4 \\ y_{k+1} = y_{k+1}^4 + \frac{h}{2} \cdot B_{1y} \left(x_{k+1}^4, \frac{y_{k+1}^4 + y_{k+1}}{2}, \frac{z_{k+1}^4 + z_{k+1}}{2} \right) \\ z_{k+1} = z_{k+1}^4 + \frac{h}{2} \cdot B_{1z} \left(x_{k+1}^4, \frac{y_{k+1}^4 + y_{k+1}}{2}, \frac{z_{k+1}^4 + z_{k+1}}{2} \right) \end{cases}$$

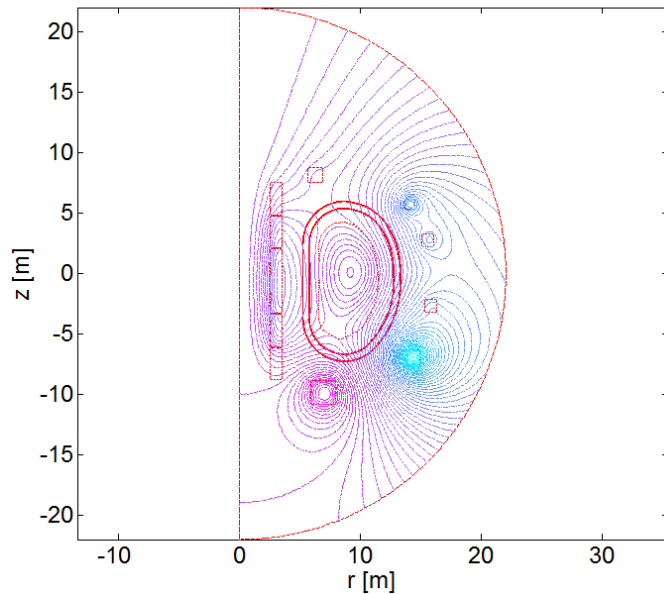
Consistent with:

$$\dot{\mathbf{x}} = \dot{\mathbf{x}}_1 + \dot{\mathbf{x}}_2 + \dot{\mathbf{x}}_3$$

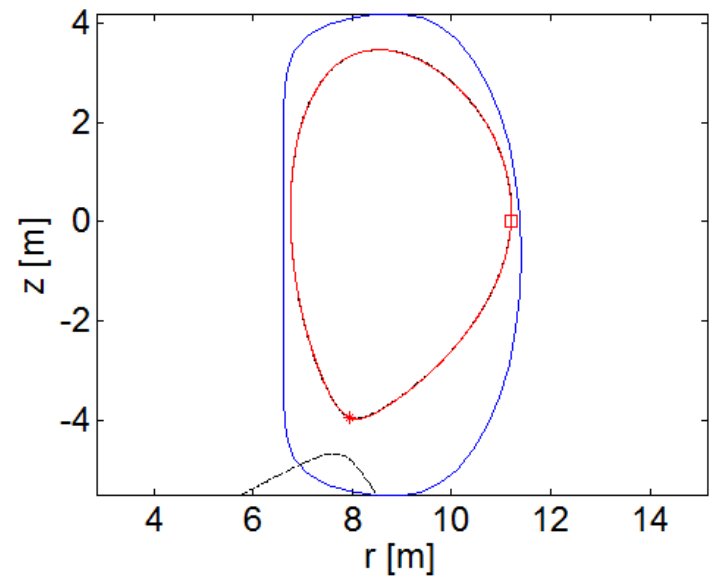
Test Case: DEMO Single-Null Divertor



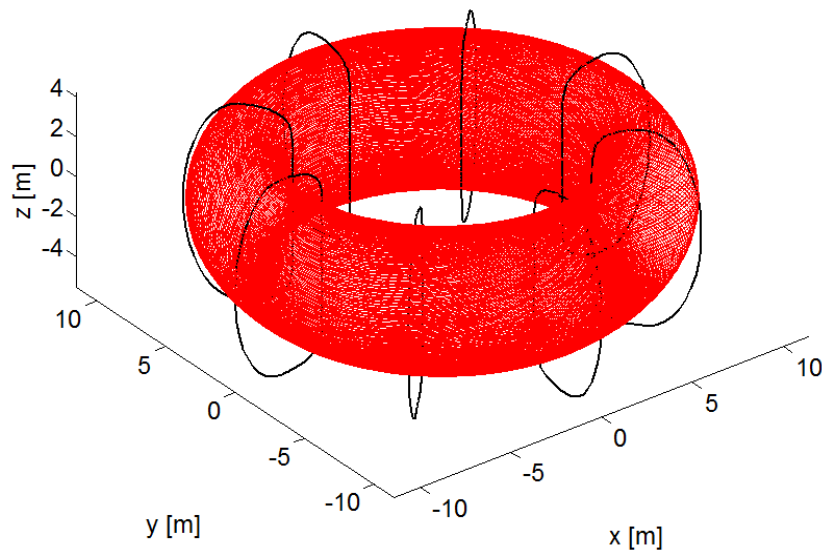
Flux Density Field Distribution



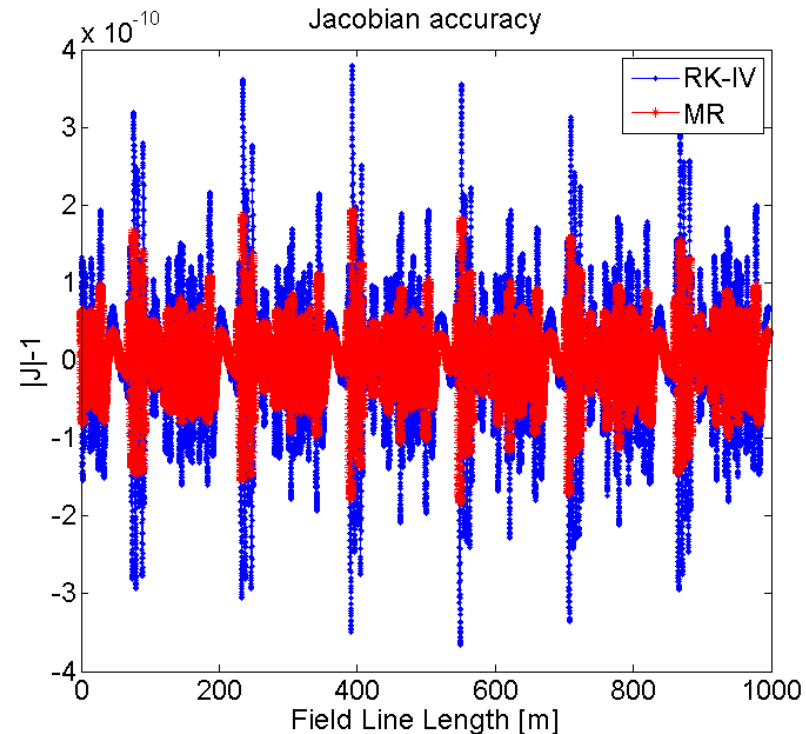
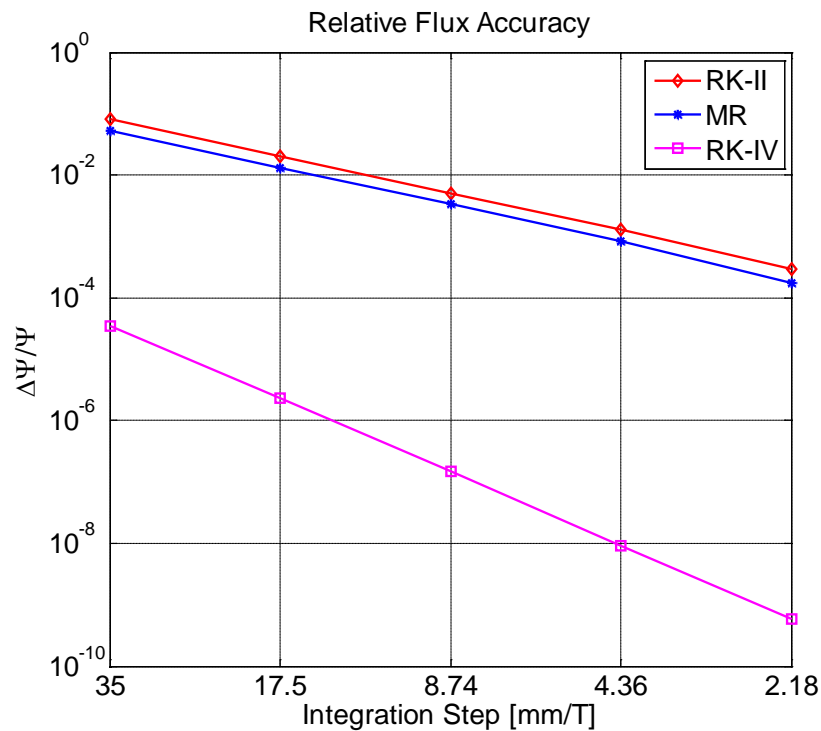
Projections on poloidal cross section, $\phi=0$



Field lines - 3-D view



MR vs RK: Performances comparison



$$\frac{J(\tau)}{J(0)} = 2 \frac{J_{\frac{h}{2}}(\tau)}{J_{\frac{h}{2}}(0)} - \frac{J_h(\tau)}{J_h(0)} + O[h^2]$$

$$\begin{cases} [|J| - 1]_{RK-IV} = 3,302 \cdot 10^{-12} \\ [|J| - 1]_{MR} = 0,460 \cdot 10^{-12} \end{cases}$$

Clebsch Decomposition for a divergence-free field



Helmholtz Theorem: Let \mathbf{F} be any continuous vector field with continuous first partial derivatives. Then \mathbf{F} can be expressed in terms of the negative gradient of a scalar potential and the curl of a vector potential.

$$\mathbf{F} = -\nabla\Phi + \nabla \times \mathbf{A}$$

If \mathbf{F} is divergence-free, so as the magnetic flux density field:

•

$$\mathbf{F} = \nabla \times \mathbf{A}$$

Choosing: $\mathbf{A} = U\nabla V$, we get:

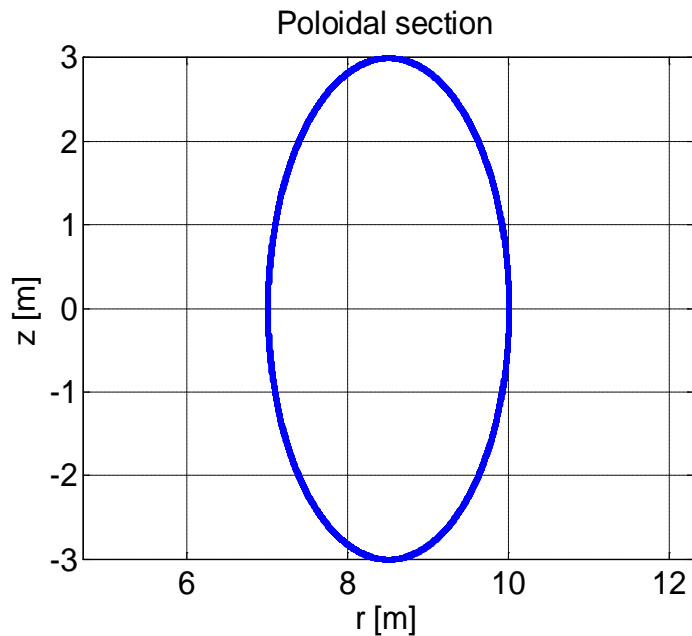
$$\mathbf{F} = \nabla \times (U\nabla V) = \nabla U \times \nabla V$$

U and V are called
Clebsch Potentials and are
analytical invariants!

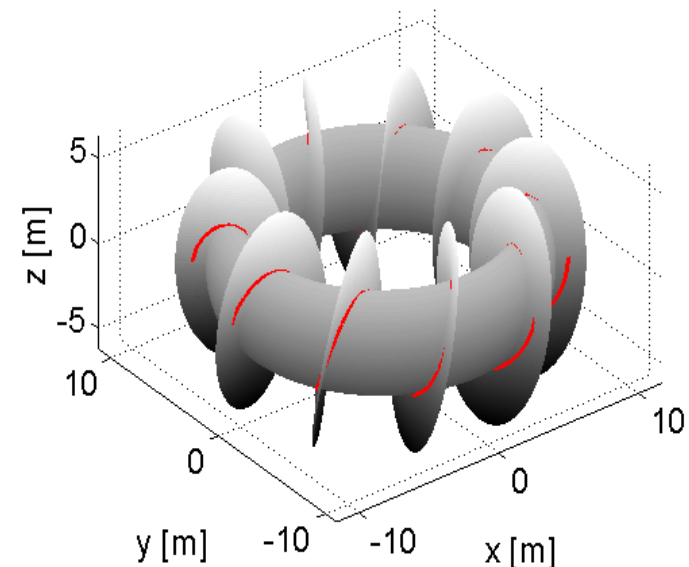
$$\mathbf{F} \cdot \nabla U = \nabla U \times \nabla V \cdot \nabla U = 0$$

$$\mathbf{F} \cdot \nabla V = \nabla U \times \nabla V \cdot \nabla V = 0$$

$$\begin{cases} U = \left(\frac{r - R_0}{a} \right)^2 + \left(\frac{z - Z_0}{b} \right)^2 + U_0 \\ V = \varphi - q\theta + V_0 \end{cases}$$



$U = \text{const.}$ & $V = \text{const.}$ Clebsch surfaces

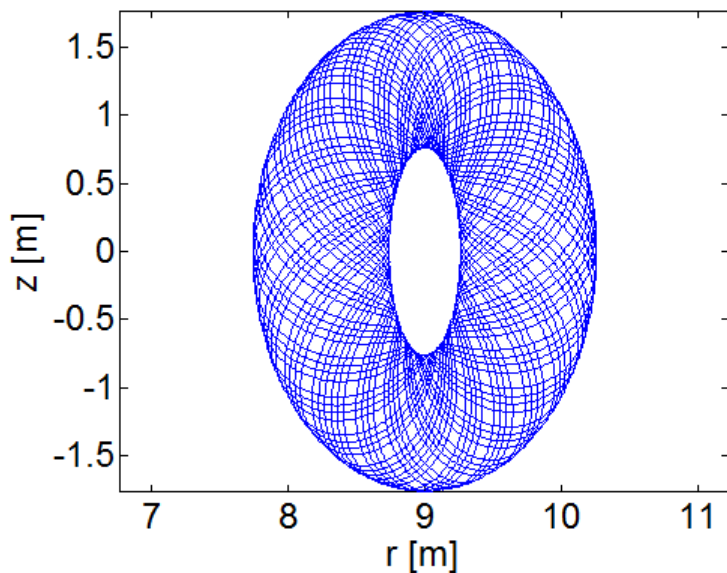


Clebsch Potentials: Non-Axisymmetric (HUGE) Ripple

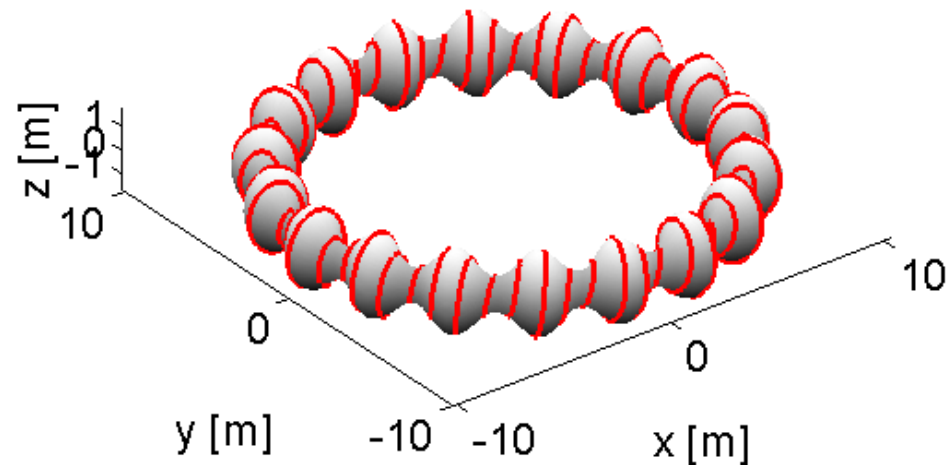


$$\begin{cases} U = \left(\frac{r - R_0}{a + \delta \cos(n\varphi)} \right)^2 + \left(\frac{z - Z_0}{b + \delta \cos(n\varphi)} \right)^2 + U_0 \\ V = \varphi - q\theta + V_0 \end{cases}$$

Global Perturbation



Global Perturbation

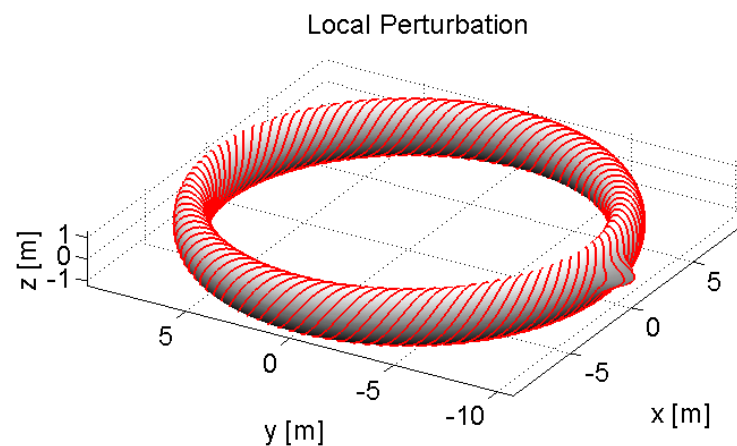
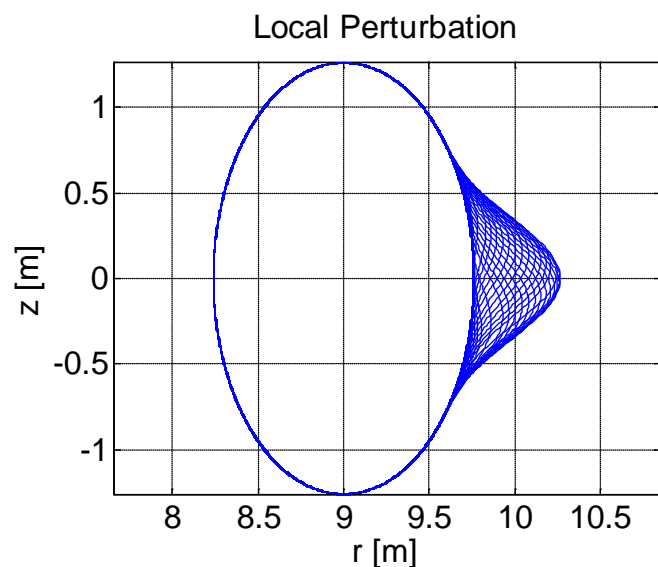


Clebsch Potentials: Non-Axisymmetric field with Local Perturbation



$$\left\{ \begin{array}{l} U = \frac{(r - R_0 - \delta U)^2}{a^2} + \frac{(z - Z_0)^2}{b^2} - 1 \\ \delta U = \delta r \cdot e^{\frac{a_1}{\Delta z} - \frac{a_1}{\sqrt{\Delta z^2 - (Z_1 - z)^2}}} \cdot e^{\frac{\alpha}{\Delta \varphi} - \frac{1}{\sqrt{\Delta \varphi^2 - (\varphi_1 - \varphi)^2}}} u(r - R_0) \text{ in } \Omega_p \text{ and } 0 \text{ elsewhere} \\ V = \theta - \frac{\varphi}{q} + V_0 \end{array} \right.$$

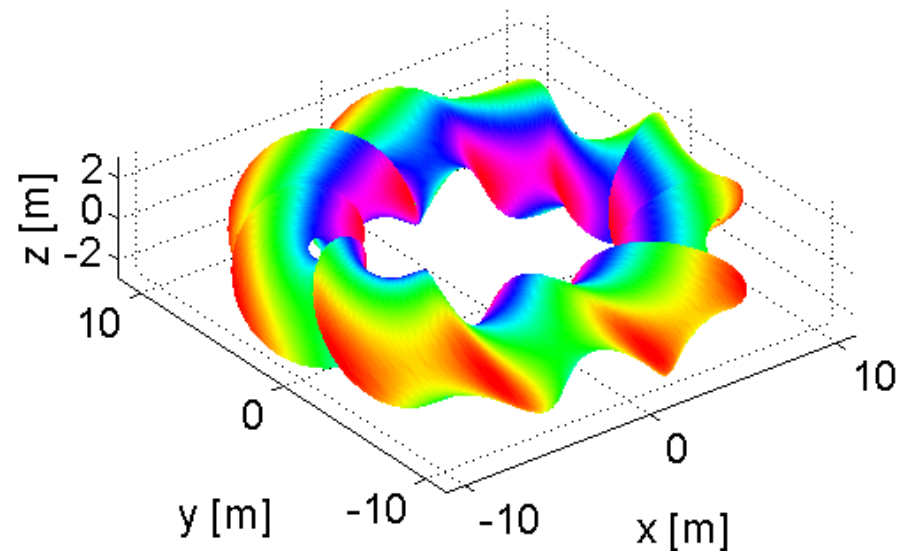
$$\Omega_p = \left\{ \begin{array}{l} |z| \leq z_1 \\ |\varphi - \varphi_1| \leq \Delta \varphi \end{array} \right\}$$



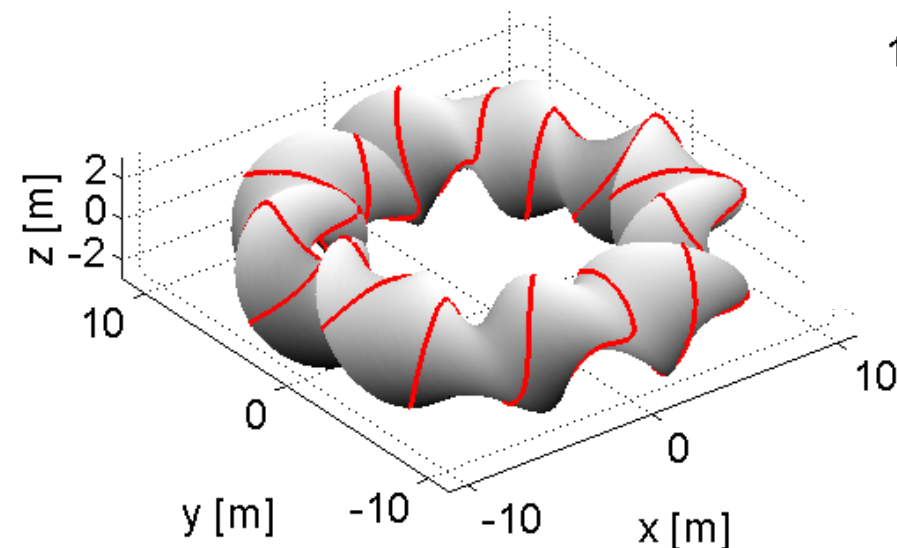
Clebsch Potentials: Stellarator Plasma

$$\begin{cases} U = \left(\frac{r \cos(n\varphi) + z \sin(n\varphi) - R_0}{a + \delta \cos(n\varphi)} \right)^2 + \left(\frac{z \cos(n\varphi) - r \sin(n\varphi)}{b + \delta \cos(n\varphi)} \right)^2 \\ V = \varphi - q\theta + V_0 \end{cases}$$

Stellarator Plasma



Stellarator Plasma



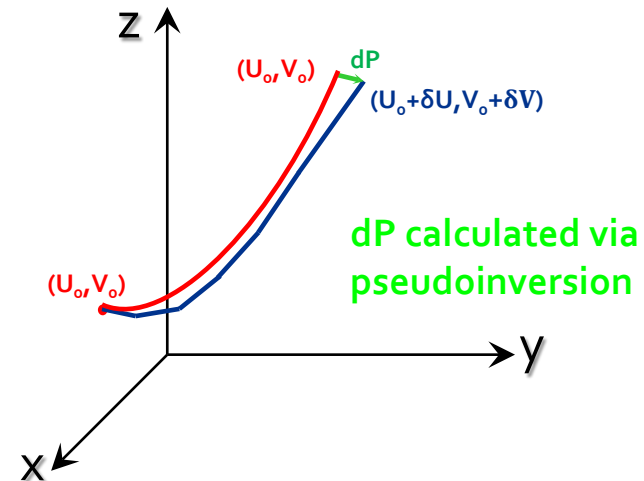
MR vs RK for 3-D vector fields



	$ U-U_0 /U_0$		$ V-V_0 /V_0$		dP [m]	
	GP	LP	GP	LP	GP	LP
MR	4.4e-1	3e-3	2.3e-1	2.0e-2	1.5e-2	8.0e-4
RK-II	2.1e-3	8.0e-4	2.0e-4	4.0e-4	1.0e-4	4.6e-5
RK-IV	4.3e-8	1.0e-7	2.0e-9	5.3e-9	4.0e-9	5.5e-9

$$GP: \begin{cases} [|J| - 1]_{RK-IV} = 0,3190 \cdot 10^{-11} \\ [|J| - 1]_{MR} = 0,4918 \cdot 10^{-11} \end{cases}$$

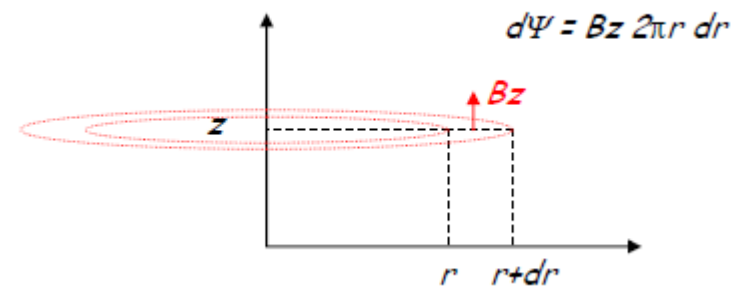
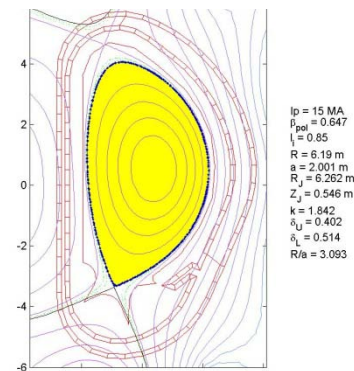
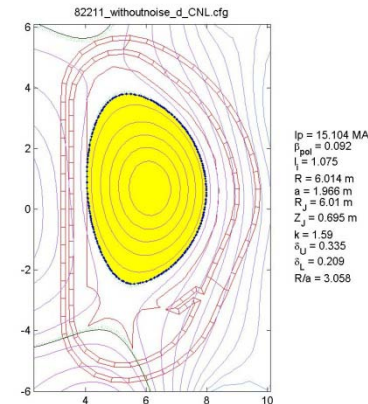
$$LP: \begin{cases} [|J| - 1]_{RK-IV} = 0,1268 \cdot 10^{-11} \\ [|J| - 1]_{MR} = 0,1027 \cdot 10^{-11} \end{cases}$$



Standard fixed step integrators are well suited for flux density field line tracing in Tokamaks

Plasma boundary and plasma-wall gaps 1/2

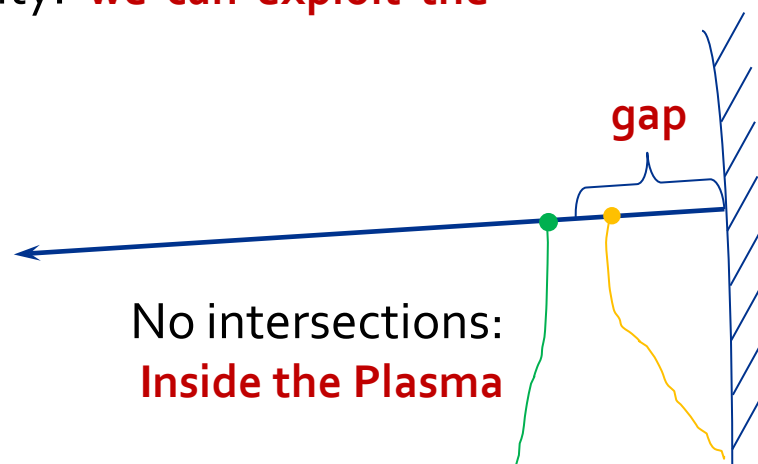
- Plasma confined in the region where the field lines do not touch the first wall
- Separatrix easily calculable in 2-D axisymmetric cases, both in limited and diverted configurations
- In 2-D axisymmetric cases, the plasma-wall gap is the distance between the intersection of the normal unit vector and the level flux line with $\Psi = \Psi_b$
- In 3-D configurations it is not possible to refer to the poloidal flux: by definition, it is an axisymmetric quantity



Plasma boundary and plasma-wall gaps 2/2

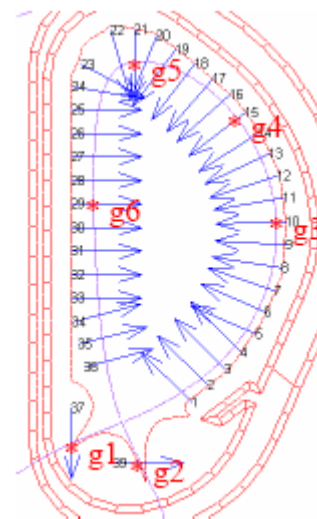


In 3-D configurations it is not possible to refer to the poloidal flux that is an axisymmetric quantity: **we can exploit the 3D field lines tracing!**



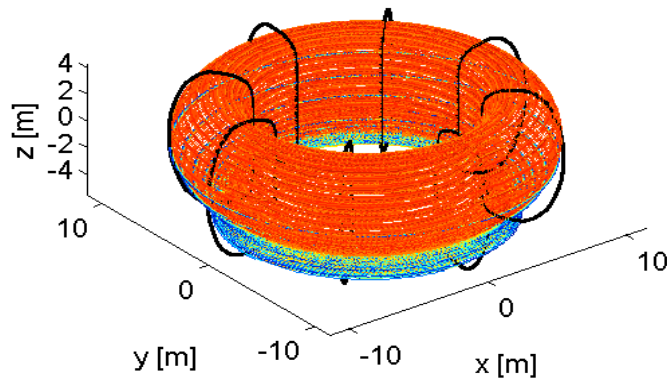
An high precision is necessary to state if a field line intersects the wall or it does not: the field line does not intersect the wall if it is closed or when it returns close to the start point at a very low distance

Intersections with the wall:
Outside the Plasma

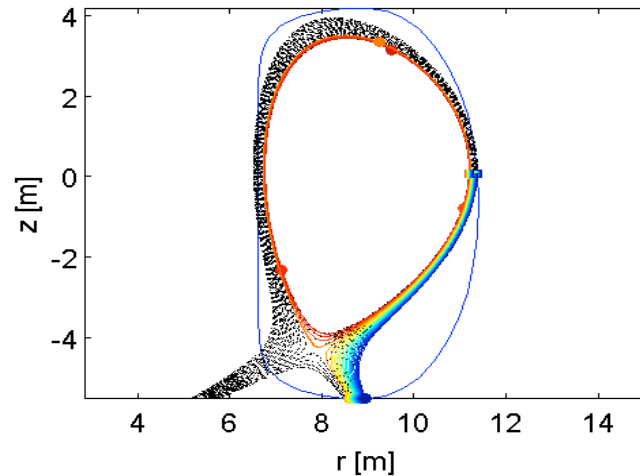


Plasma Boundary Reconstruction 1/5

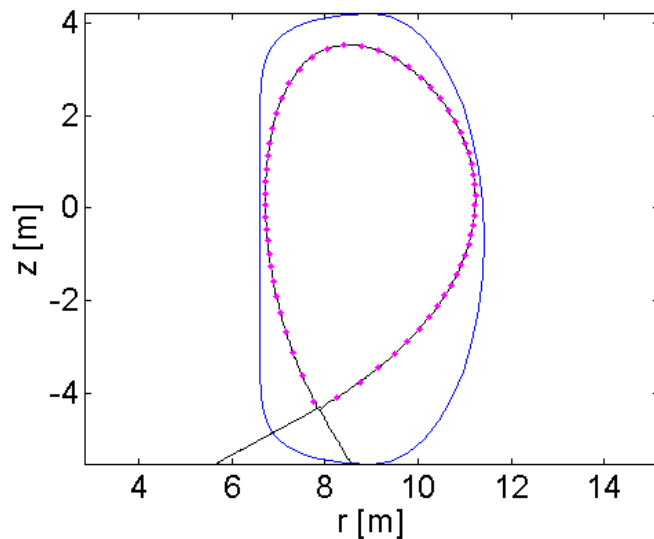
Field lines - 3-D view



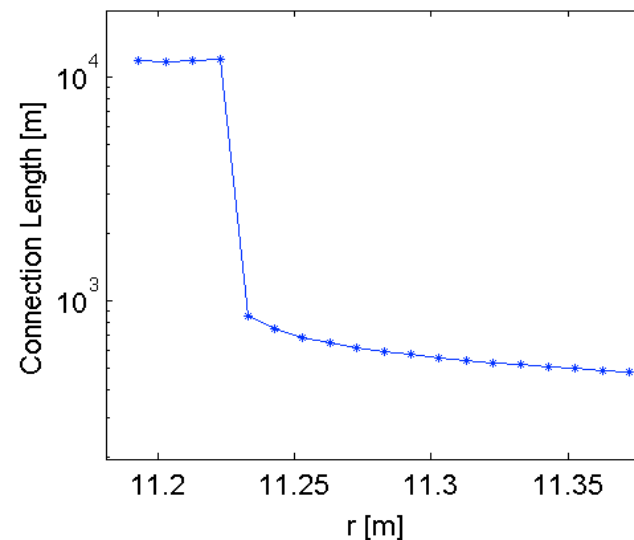
Poloidal cross section, $\phi=0$



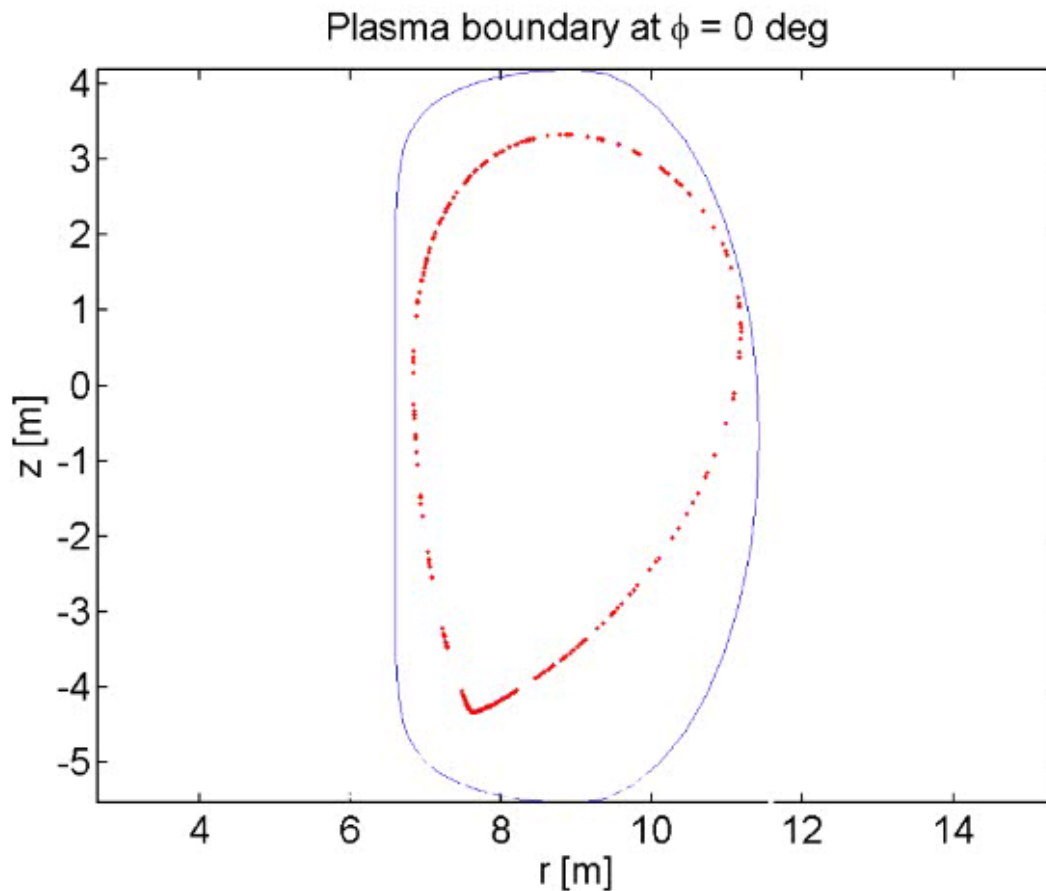
Plasma Boundary Reconstruction



Connection Length vs Radial coordinate



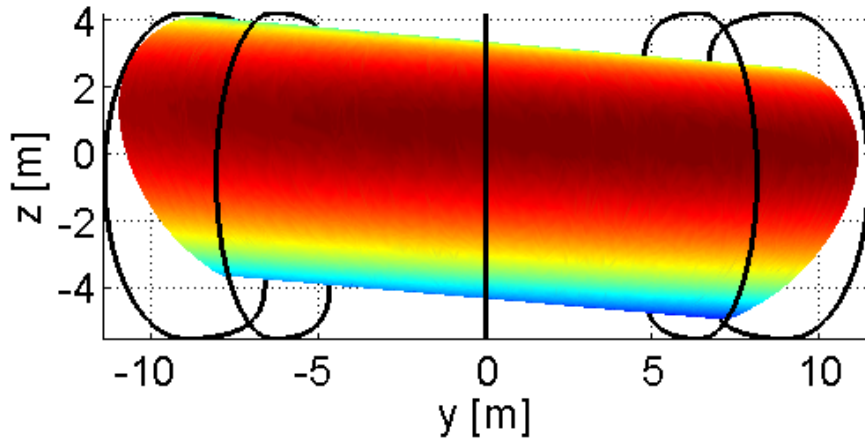
Plasma Boundary Reconstruction 2/5



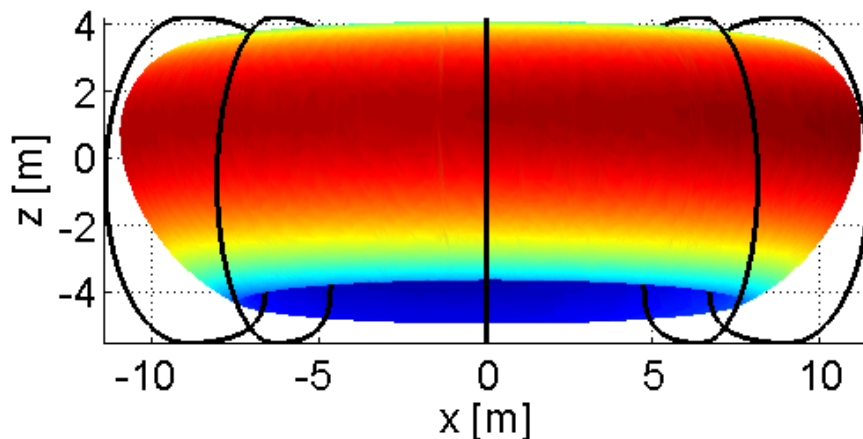
Effect of the plasma kink: $\rho_x = 10$ cm, $\vartheta_x = 5$ deg

Plasma Boundary Reconstruction 3/5

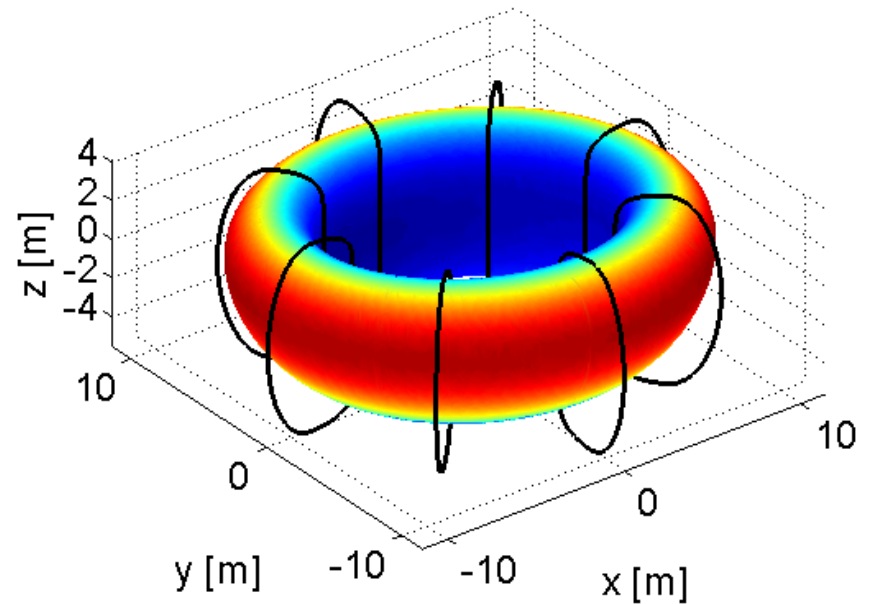
3-D Plasma Boundary



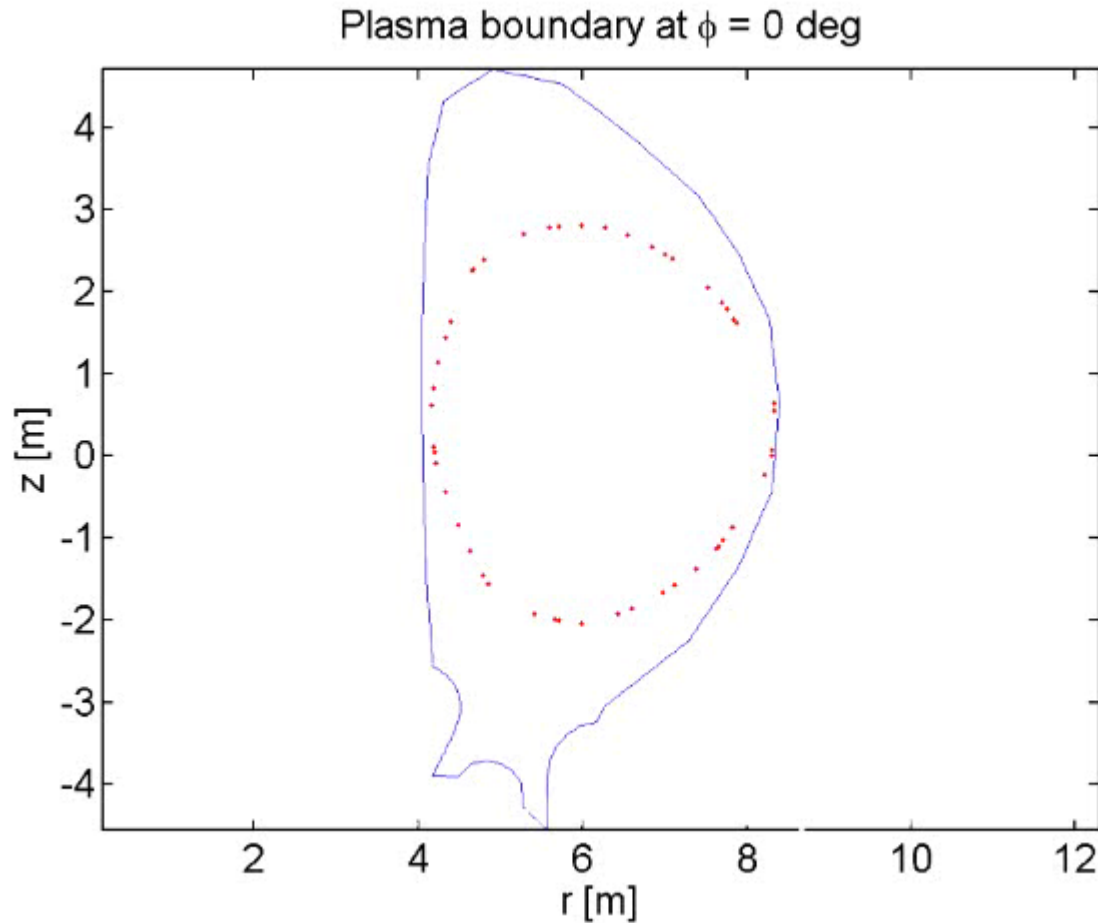
3-D Plasma Boundary



3-D Plasma Boundary



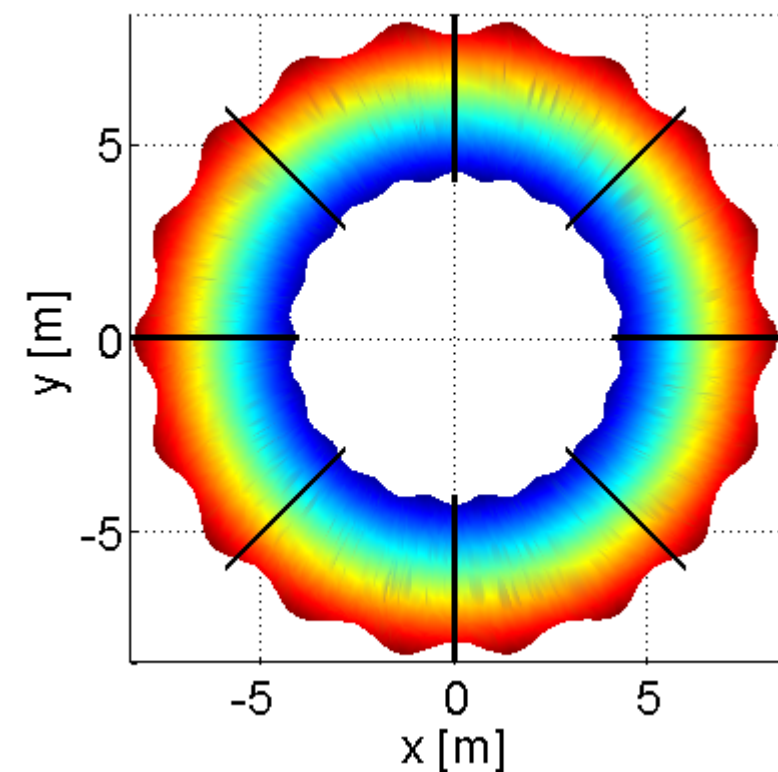
Plasma Boundary Reconstruction 4/5



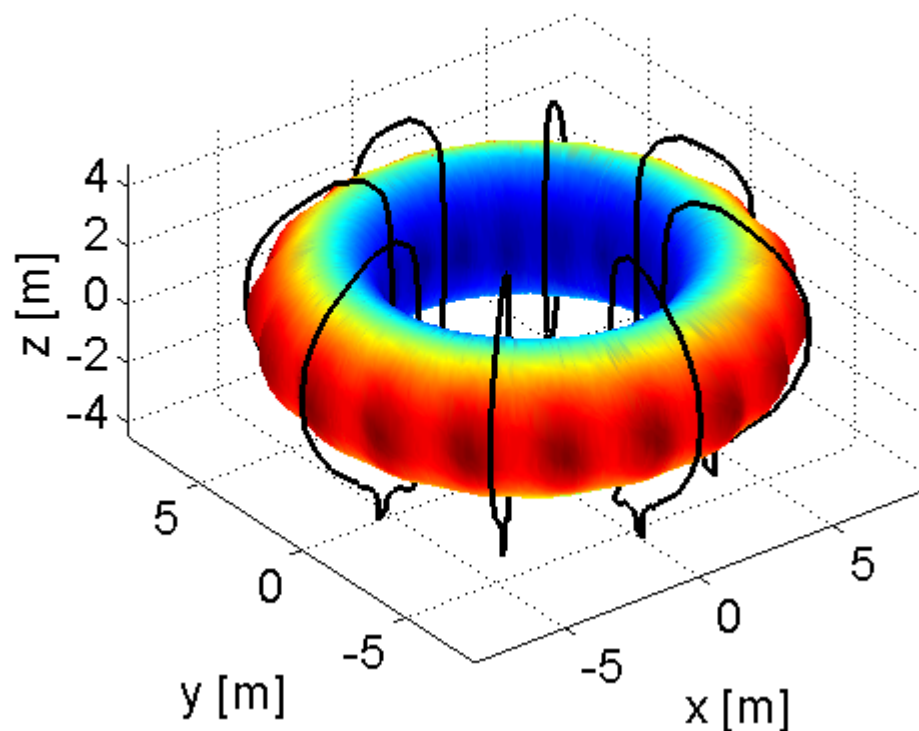
Effect of a (HUGE) Toroidal Field Coils Ripple

Plasma Boundary Reconstruction 5/5

3-D Plasma Boundary



3-D Plasma Boundary



- Nuclear fusion energy has been introduced, depicting the physics and its engineering features.
- Two techniques for three-dimensional flux density field identification has been.
- The first technique is based on the superposition of an equivalent set of axisymmetric filamentary currents and magnetic dipoles.
- The second technique is based on the decomposition of the identification problem into the axisymmetric and non-axisymmetric sub-problems:
 - The axi-symmetric part in the poloidal plane is solved with a basis function decomposition whose b.c. are given by a Fourier expansion along the VIW and VEW
 - The toroidal non axi-symmetric component is expanded with a Fourier representation along φ -direction, whose coefficients are functions of the poloidal coordinates and are calculated as before
- Preliminary analyses demonstrated how such schemes are able to deal with a significant class of 3D perturbations, thanks to its flexibility.

- Several test cases have been identified with a precision every time better than one percent
- New classes of basis functions and the exploitation of information of other sensors (e.g. full flux loops, saddle loops, ...) are under evaluation at present.
- The problem of 3D field line tracing has been discussed. Comparing standard integrators and volume preserving integrators, we can say that Fixed-Step Fourth Order Runge-Kutta Integrator:
 - is well suited for field line tracing in fusion tokamaks;
 - is more accurate w.r.t. Mid-Point Rule;
 - preserves the solenoidal structure of the ODE set as well as the Volume-Preserving Mid-Point Rule, showing to be well suited for long integration.
- A new fast and accurate way to calculate the plasma-wall gap and to reconstruct the shape in axisymmetric and non-axisymmetric plasmas has been presented.

Thank You for
Your Kind
Attention



QUESTIONS
COMMENTS
CONCERNS